universität wien

MASTERARBEIT | MASTER'S THESIS

Titel | Title

Evaluation of AlphaFold Models of Cav2.x Channels Using Experimental Functional Data

verfasst von | submitted by

Denis Josipovic BSc

angestrebter akademischer Grad | in partial fulfilment of the requirements for the degree of

Magister pharmaciae (Mag. pharm.)

Wien | Vienna, 2026

Studienkennzahl lt. Studienblatt | Degree programme code as it appears on the student record sheet:	UA 066 605
Studienrichtung lt. Studienblatt | Degree programme as it appears on the student record sheet:	Masterstudium Pharmazie
Betreut von | Supervisor:	Assoz. Prof. Mag. Dr. Anna Weinzinger Privatdoz.

Acknowledgements

First and foremost, I would like to express my deepest gratitude to Assoc.-Prof. Mag. Dr. Anna Weinzinger, Privatdoz., for accepting me into her research group and for her supervision throughout this master's thesis. I'm very grateful for having experienced computational work in her team. I also want to express my deepest gratitude to Ilia Steshin, who was available 24/7 for help and or input, spending many hours helping me, no matter what time of day. I also want to thank my family and friends for the constant support and motivation provided by them, helping me push through any adversity along the way. A special thanks goes out to my university friend group, having built a tight network of unconditional support and help for each other, knowing each other's struggles very well from personal experience, and for spending countless hours studying together and motivating each other to keep going. Every challenge along the way was faced as a team, increasing the chances of prevailing. Without the people mentioned above, none of this would have been possible and I'm deeply grateful for every one of them.

Abstract

The rare disease GNB1 encephalopathy (GNB1-E) is caused by different genetically created mutations of Gβ1, with epilepsy being one of the symptoms. Because Cav2.x channels play a key role in controlling neuronal signalling and are regulated by Gβγ subunits, they represent a potential therapeutic target in GNB1-E-associated epilepsy. The aim of this thesis is to assess whether AlphaFold predictions of Cav2.x channel structures are consistent with available experimental evidence and can therefore be used for further molecular dynamics (MD) studies. Cryo-EM structure availability for these channels is very limited, hence AlphaFold predictions could be used for MD simulations instead. In order to assess the validity of the AlphaFold predictions, this thesis compares them with evidence from experimental data.

Cav2.2 has the most experimental data, which also overlaps with the AlphaFold prediction to a great extent. An N-terminal α-helix that has been proven to be essential for Gβ1γ2 mediated inhibition is identified as the main Gβ1γ2 binding site in Cav2.2 by AlphaFold. The N-terminus of Cav2.2 in general is also proven to drastically impact Gβ1γ2 mediated inhibition when inserted into Cav2.3.

The formation of a Gβγ-binding-pocket is not demonstrated by AlphaFold (which is a static structural prediction), but combining the knowledge extracted from the prediction with the knowledge from experimental data insinuates it. Potentially this could be observed in MD simulations, as they are mobile simulations whereas AlphaFold is a static structural prediction.

Cav2.3 seems to differ drastically from Cav2.1 and Cav2.2 when it comes to Gβγ mediated inhibition and AlphaFold fails to confidently predict its supposed main Gβγ binding site, the C-terminus.

In conclusion this thesis provides a comparison of experimental data and AlphaFold predictions and their theoretical validation or invalidation.

Zusammenfassung

Die seltene Erkrankung GNB1 Enzephalopathie (GNB1-E) wird durch verschiedene genetisch hervorgerufene Mutationen in Gβ1 verursacht, wobei Epilepsie eines der Symptome ist. Da Cav2.x Kanäle eine Schlüsselrolle in der neuronalen Signalübertragung spielen und von den Gβγ Untereinheiten reguliert werden, stellen sie ein potenzielles Ziel für die medikamentöse Behandlung von GNB1-E assoziierter Epilepsie dar. Das Ziel dieser Masterarbeit ist es zu bewerten ob die strukturellen AlphaFold Vorhersagen mit den Ergebnissen struktureller Experimente übereinstimmen und daher für Molekulardynamik(MD)-Simulationen verwendet werden können. Da die Verfügbarkeit von Kryo-EM Strukturen dieser Kanäle sehr begrenzt ist, könnten stattdessen AlphaFold-Vorhersagen für MD-Simulationen verwendet werden. Um die Validität der AlphaFold-Vorhersagen zu bewerten, vergleicht diese Arbeit sie mit experimentellen Daten.

Cav2.2 verfügt über die umfangreichsten experimentellen Daten, die zudem in hohem Maße mit den AlphaFold Vorhersagen übereinstimmen. Eine N-terminale α-Helix, die als essenziell für die durch Gβ1γ2 vermittelte Inhibition nachgewiesen wurde, wird von AlphaFold als primäre Gβ1γ2 Bindestelle in Cav2.2 identifiziert. Der N-Terminus von Cav2.2 als Ganzes beeinflusst erwiesenermaßen die Gβ1γ2 vermittelte Inhibition drastisch wenn er in Cav2.3 eingesetzt wird.

Die Bildung einer Gβγ Bindungstasche wird durch AlphaFold (eine statische Strukturvorhersage) nicht gezeigt, jedoch deutet die Kombination der aus der Vorhersage gewonnenen Erkenntnisse mit experimentellen Daten darauf hin. Potenziell könnte dies in MD-Simulationen beobachtet werden, da diese dynamisch sind, während AlphaFold eine statische Vorhersage liefert.

Cav2.3 scheint sich hinsichtlich der Gβγ vermittelten Inhibition deutlich von Cav2.1 und Cav2.2 zu unterscheiden, und AlphaFold gelingt es nicht, die mutmaßliche Hauptbindestelle für Gβγ, den C-Terminus, mit hoher Zuverlässigkeit vorherzusagen.

Zusammenfassend bietet diese Arbeit einen Vergleich zwischen experimentellen Daten und AlphaFold Vorhersagen sowie deren theoretische Validierung oder Infragestellung.

Table of contents

Inhalt

List of abbreviations

ADHD	attention deficit and hyperactivity disorder
AID	alpha interaction domain
ABP	AID-binding pocket
AF	Alphafold
AMPA	α-amino-3-hydroxy-5-methyl-4-isoxazole propionic acid
ASD	autism spectrum disorder
BID	beta interaction domain
CACNA1A	α subunit of Cav2.1
CACNA1B	α subunit of Cav2.2
CACNA1E	α subunit of Cav2.3
CALM1/CaM1	calmodulin 1
CALM2/CaM2	calmodulin 2
CALM3/CaM3	calmodulin 3
CDI	Ca2+ dependent inactivation
CDF	Ca2+ dependent facilitation
CMA	chromosomal microarray analysis
DD	developmental delay
EEG	electroencephalogram
GBP	Gβγ binding pocket
GI	gastrointestinal
GDD	global development delay
GDP	guanosine diphosphate
GIRK	G-protein gated inwardly rectifying potassium channels
HVA	high voltage activated channels
SH3	Src homology 3 domain
GNB1	G-protein subunit beta 1
GNB1-E	GNB1 encephalopathy
GNB2	G-protein subunit beta 2
GNB3	G-protein subunit beta 3
GNB4	G-protein subunit beta 4
GNB5	G-protein subunit beta 5
GNG2	G-protein subunit gamma 2
GOF	gain of function
GPCR	G-protein-coupled receptor
GTP	guanosine triphosphate
ID	intellectual disability
LOF	loss of function
MRI	magnetic resonance imaging
N/OFQ	nociceptin/orphanin FQ
NOP	nociceptin opioid receptor
PPF	Prepulse facilitation
RTK	receptor tyrosine kinase
TARP	transmembrane AMPA receptor regulatory protein
VDA	voltage dependent activation
VDI	voltage dependent inhibition
VSD	voltage sensing domain

List of figures

Introduction

1.1 GNB1 encephalopathy (GNB1-E)

The gene GNB1 codes for the guanine nucleotide-binding protein subunit beta-1 (Gβ1) which is broadly present in the human body (Petrovski et al. 2016).

GNB1 encephalopathy (GNB1-E) is a rare neurodevelopmental disorder, with only a limited number of genetically confirmed cases reported worldwide.

It is caused by pathogenic mutations in GNB1 (G-protein beta subunit 1) leading to altered Gβγ function and disruption of G-protein-mediated signalling pathways. This disrupts GPCR-mediated neuronal communication, resulting in developmental delay (DD), intellectual disability (ID), epilepsy, hypotonia, eye-movement- and movement disorders and visual- and hearing impairment. Behavioral symptoms like attention deficit and hyperactivity disorder (ADHD) or autism spectrum disorder (ASD) can also appear. GNB1-E can appear as both a de novo germline mutation, as well as an inherited mutation, although the prior is currently far more prevalent (Nasvytis et al. 2024).

Although there is a multitude of symptoms, the one consistently reported is global development delay (GDD). Other symptoms that are statistically likely are epilepsy, ID, gastrointestinal- (GI) and muscle-tone abnormalities as well as abnormal vision (Da Silva et al. 2021).

1.1.1 Pathogenesis

GPCRs are responsible for a large amount of biologic functions, being located in a wide array of tissues in the human body and being coded for by hundreds of human genes. They translate extracellular signals into intracellular G-protein mediated signalling cascades by activating said G-proteins. These G-proteins are heterotrimers consisting of an α subunit, a β subunit and a γ subunit. Each of these subunits can be part of the heterotrimer in a variety of versions as there are 16 different α subunits, 5 different β subunits and 13 different γ subunits of G-proteins. The α subunit is not just bound to Gβγ but also to GDP. After the activation of GPCRs the trimer binds the GPCR intracellularly, where the GDP-GTP exchange takes place. This exchange causes a separation of the heterotrimer into Gα-GTP and a Gβγ heterodimer, which then proceed to partake in different signalling cascades independently from each other. Neuronal excitability is regulated by Gαβγ subunits via their direct regulation of neuronal ion-channels or via second messenger pathways (Fig. 1) (Wootten et al. 2018; Nasvytis et al. 2024).

A mutated Gβ1 can affect Gβγ mediated signalling in multiple ways. Many pathogenic GNB1 variants are located within the switch interface, where they can alter interactions with Gα subunits and downstream effectors. Gβ1 mutations can affect binding of Gα or downstream effectors and cause

GoF (gain of function) or LoF (loss of function) for downstream effectors (Petrovski et al. 2016). Furthermore they can affect Gβγ stability and Gαβγ binding to the GPCRs (G-protein-coupled receptors) (Lohmann et al. 2017).

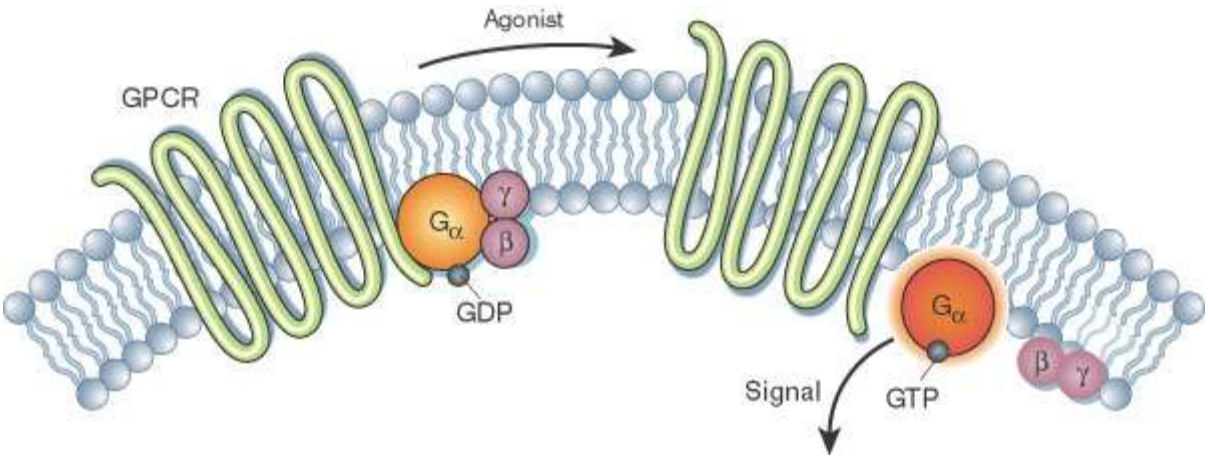

Figure 1 GPCR-Gαβγ activation

Dissociation of Gα-GTP and Gβγ dimer after GDP-GTP exchange on the intracellular side of the GPCR (https://www.nature.com/scitable/topicpage/gpcr-14047471/)

1.1.2 Clinical manifestation

GNB1-E is a clinically heterogeneous neurodevelopmental disorder in which 100% of the affected individuals show GDD, often accompanied by moderate to severe ID. A substantial proportion of patients show significant motor impairment, with many unable to achieve independent walking. In addition to these core features, a range of neurological manifestations may occur, including epilepsy, hypotonia, movement abnormalities, and disturbances of ocular or sensory function. Some individuals also exhibit structural brain changes, as well as behavioural issues, feeding difficulties and involvement of other organ systems such as gastrointestinal abnormalities or structural defects of the urinary tract and reproductive organs (Revah-Politi et al., n.d.).

GDD can be seen in every patient but it does not necessarily show right after birth. Early in life it only makes itself noticeable through difficulty of feeding which also results in growth delay, while children who grow older show increasingly more evident developmental delays. Motor development is particularly affected, with many individuals showing delayed or absent onset of walking. Those who do walk often exhibit instability and are therefore prone to fall. Hemiplegia, spastic diplegia, or dyskinetic quadriplegia are also known to appear. Limited or absent speech is also common, especially when it comes to expression. Understanding of spoken or written words is less affected than formulating them oneself (Nasvytis et al. 2024).

Three quarters of patients suffer from ID in varying extent. Reduced muscular and cerebral volume with delayed myelination impact both physical and mental activity, as well as the neuronal system. These conditions increase susceptibility to epilepsy and seizures, which appear in multiple forms in GNB1-E patients: focal, tonic, myoclonic, generalized tonic-clonic and epileptic absence. Sensory impairments appear both visually and acoustically (Revah-Politi et al., n.d.).

Behavioral impairments include repetitive behaviors as well as ADHD and ASD. Organs can also be affected in multiple forms like GI problems, cardiovascular abnormalities, hypothyroidism, cutaneous mastocytosis and craniofacial anomalies (Revah-Politi et al., n.d.).

1.1.3 Prognosis

Because most individuals diagnosed with GNB1 encephalopathy are still children or young adults, estimating life expectancy is currently not possible with confidence. However, reported adult cases confirm that long-term survival can occur. The scarcity of longitudinal data limits any definitive conclusions regarding prognosis, and current understanding remains largely descriptive. Ongoing clinical care and multidisciplinary support appear to play an important role in long-term functional stability, but the overall impact of the condition on lifespan has yet to be clearly defined (Nasvytis et al. 2024).

1.1.4 Diagnosis and assessment

GNB1-mutations can be identified via DNA-sequencing but identifying a mutation does not necessarily mean that the source has been identified. GNB1-mutations L30F, H91R, and K337Q for example have been found to be benign (Lohmann et al. 2017).

Since currently no laboratory markers have been identified as viable for diagnosis of GNB1-E, genetic testing remains the only viable option. Chromosomal microarray analysis (CMA) is the primary choice, followed by next generation sequencing in case of an inconclusive result. (Nasvytis et al. 2024)

Due to potential reduction of brain- and muscle, MRI (magnetic resonance imaging) is encouraged. The same goes for EEG (electroencephalogram) due to potential abnormal brain activity and seizures (Nasvytis et al. 2024).

1.1.5 Treatment

GNB1-E induced seizures are mostly treated with antiepileptic drugs but there is no specific guideline for treating GNB1-E. The most promising antiepileptic drug according to animal trials is ethosuximide. GNB1-E induced movement disorders are currently being treated with dopamine-related medications, anticholinergics, benzodiazepines and baclofen but no option is ideal due to side effects and limited success (Nasvytis et al. 2024).

1.2 Gβγ dimer structure

The β subunits form a β-propeller consisting of seven blades, each built from four antiparallel β-strands. The first N-terminal residues form an α-helix that associates closely with the γ subunit, creating stability for the Gβγ complex (Fig. 2) (Smrcka 2008).

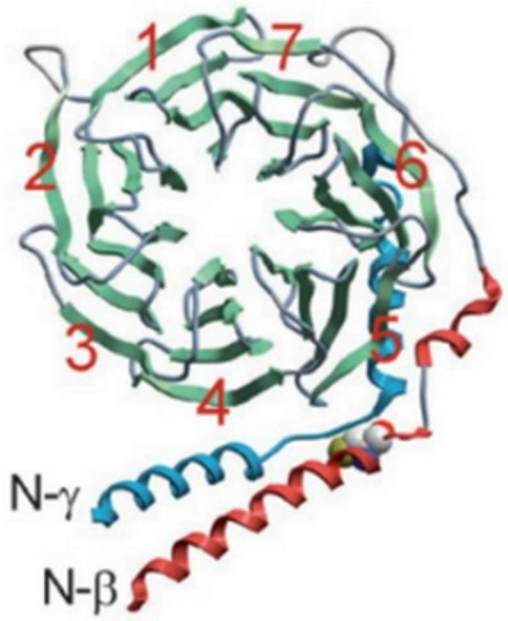

Figure 2 Gβγ strucure

3D structure of the Gβγ dimer. Gβ is pale green with its N-terminal helix in red and Gγ is blue. The 7 blades of the β-propeller are numbered by red numbers 1-7 (Smrcka 2008).

A number of residues of Gβ bind Gα and they are separated into 2 groups, the N-terminal group and the switch interface (Figs. 3 and 4):

- N-terminal residues: L55, K78, I80 and I89
- Switch interface residues: K57, Y59, S98, W99, M101, L117, N119, T143, D186, D228, W332 (Ford et al. 1998).

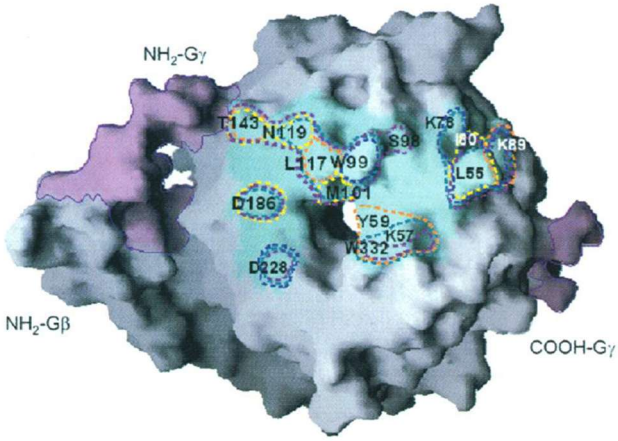

Figure 3 Switch interface

Model of Gβγ that represents the Gα binding area of Gβ. Gβ is gray, Gγ is pink and the region of Gβ that can bind Gα is green. The specific residues are marked and numbered (Ford et al. 1998).

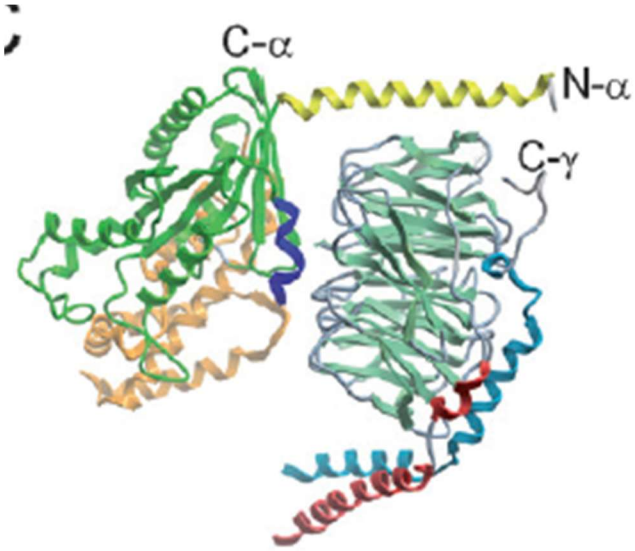

Figure 4 Gαβγ

Gα is green with a yellow N-terminus and a dark blue Switch II area, Gβ is pale green with a red N-terminus and Gγ is blue. The switch interface residues of Gβ are located in its grey area that faces Gα (Smrcka 2008).

These residues were mutated to alanine via point mutation in order to observe the mutations abilities to fold heterotrimers with Gα. The ability of I80A, K89A, L117A and W332A to form heterotrimers with Gα was impacted negatively. Furthermore I80A, K89A, S98A, W99A, M101A, L117A, N119A, T143A, D186A, D228A, W332A were unable to form heterotrimers that successfully partake in light-activated GDP-GTP exchange, catalysed by rhodopsin, with the α subunit of the G-protein transducine (Gtα). Therefore some mutations that were still able to fold heterotrimers only folded trimers that were not

fully functional and the Gβγ heterodimer seems to have an active role in the GDP-GTP exchange that occurs on Gα (Ford et al. 1998).

1.3 Cav2.x channels

Voltage gated Ca2+ channels are involved in a multitude of diseases and symptomatic expressions due to their involvement in neurotransmitter release, hormone secretion, muscle contraction and gene expression. The Cav2.x family are high voltage activated channels (HVA) and mostly responsible for synaptic transmission. Cav2.1 are P/Q-type channels, Cav2.2 are N-type channels and Cav2.3 are R-type channels (Caminski et al. 2022).

P/Q-type and N-type Ca2+ channels are expressed in the synapses, where their activation leads to neurotransmitter release. (Zamponi and Currie 2013) R-type channels are mostly expressed in the brain in multiple regions. (Parajuli et al. 2012) In the central nervous system R-type channels are located at presynaptic terminals where they also contribute to neurotransmitter release (Wilson et al., n.d.).

The nociceptin opioid receptor (NOP) serves as a well-characterized example of a GPCR that modulates Cav2.x channels through Gβγ signalling. NOP and many other GPCRs have been shown to cause both voltage dependent and voltage independent inhibition of ion channels (Fig. 5). Voltage independent inhibition is potentially accomplished through activating receptor tyrosine kinases (RTK) and or protein kinases through Gα. After NOP activation via binding of nociceptin, also called orphanin FQ or N/OFQ, the characteristic GDP-GTP exchange happens and the heterotrimer dissacotiates into GTP-Gα and Gβγ. The latter then proceeds to directly inhibit voltage gated calcium channels like members of the Cav2.x family, as well as activate G-protein gated inwardly rectifying potassium channels (GIRK) and regulate a multitude of intracellular signalling pathways. Inhibition of the α subunit of Cav2.x via Gβγ directly results in decreased secretion of neurotransmitters and neuronal excitability, although the β subunit isoform of Cav2.x also affects modulation via G-proteins (Caminski et al. 2022).

Although Gβ and Gγ by themselves show little to no inhibition on Cav2.2, multiple Gβγ variants do (Gβ1γ2, Gβ1γ3 and Gβ1γ7) so directly without the involvement of second messengers. Injection of GDP-Gα results in reduced inhibition due to its binding affinity to Gβγ. Hence GPCR induced dissociation of Gαβγ into DTP-Gα and Gβγ can directly result in Cav2.2 inhibition, which shows itself in the form of slowed activation kinetics and reduced Ca2+ flow. This Gβγ mediated inhibition is voltage dependent since voltage of +80mV reduces Gβγ induced inhibition and restores Ca2+ currents (prepulse facilitation) (Ikeda 1996).

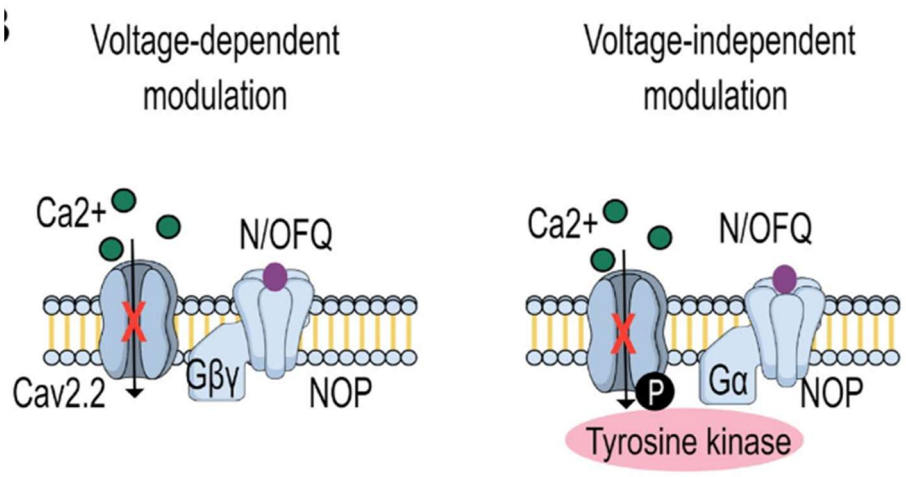

Figure 5 Voltage dependent and independent modulation via NOP activation.

Gβγ directly inhibits Cav2.2 and causes voltage dependent inhibition while phosphorylation of Cav2.2 via Gα/RTK causes voltage independent inhibition (Caminski et al. 2022).

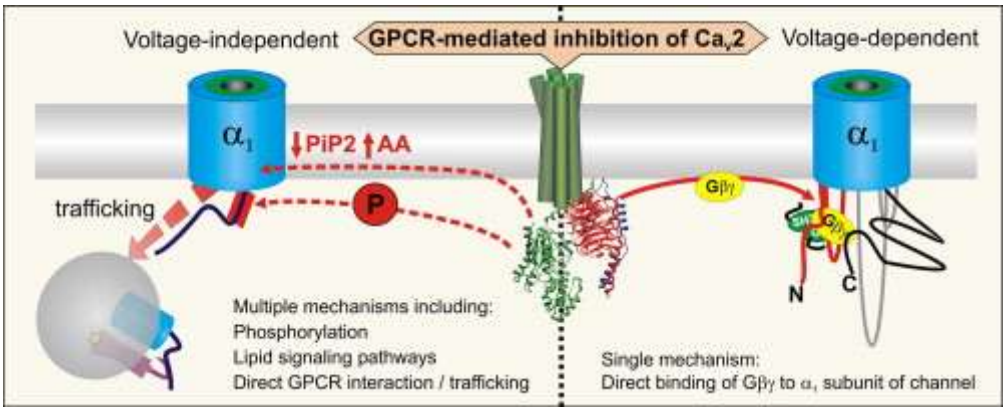

Figure 6 Voltage independent pathway.

https://doi.org/10.1016/j.bbamem.2012.10.004

Activated GPCR activates enzymes that lead to PIP2 depletion and lipid messenger (AA = arachidonic acid) production, leading to phosphorylation of the α subunit intracellularly, causing voltage independent inhibition (Zamponi and Currie 2013).

.

Inhibition of presynaptic Cav2.2 channels has been linked to potential analgesic effects by disrupting sensory transmission to the spinal cord. Knock-out mice lacking Cav2.2 channels have shown effects like reduced sensitivity to different types of pain, increased vigilance, hyper-aggression, reduced anxiety levels and reduced symptoms when in alcohol withdrawal (Cav2.2 was also linked to reward-seeking). Hence Cav2.2 is involved in a wide array of physiological effects (Caminski et al. 2022).

VDI of Cav channels affects their gating properties and does not inhibit them permanently. This is demonstrated by the 2 gating states “willing” and “reluctant”. Uninhibited channels are in the willing state, but when the inhibiting protein Gβγ binds Cav2.x channels the reluctant state is induced. In the reluctant state calcium currents are reduced because stronger depolarization is needed for channel activation and the activation and therefore channel opening are also slower. Hence reluctant channels are more unlikely to open and even when they do they open slowly. However Gβγ inhibition can be reversed by voltage, changing the gating state to willing again (Zamponi and Currie 2013).

The different Cav2.x channels can all be inhibited by Gβγ but to different extents. Out of the 3 channels, Cav2.3 is the least susceptible to Gβγ mediated inhibition. Cav2.1 and Cav2.2 are inhibited to stronger extents but differentiate in terms of Gβ1γ2 dissociation rate. Cav2.1 releases Gβ1γ2 faster while Cav2.2 retains Gβ1γ2 longer. Consequently Gβ1γ2 mediated inhibition is stronger for Cav2.2. Subsequently the strength of inhibition is Cav2.2 > Cav2.1 > Cav2.3 (Berecki et al. 2014; Zhang et al. 1996).

1.3.1 Cav2.x α subunit (CACNA1x/α1x)

The α subunit (Fig. 7) is the pore forming subunit of Cav2.x and consists of 4 transmembral domains and each domain consists of 6 α-helices (S1-S6). The first 4 helices of each domain form the VSD (voltage sensing domain 1-4) while S5 and S6 build the pore. Therefore the pore itself consists of 8 helices, 2 from each domain. VSDs I-IV all form similar shapes and or located on the outside of the pore, however they do not consist of the same amino acid sequence, therefore reacting differently to depolarization. PPF affects VSD I the most, followed by VSD III and IV, while VSD II seems to be irresponsive to voltage changes (Nilsson et al. 2024).

Despite the VSDs not having the same amino acid sequence, S4 of the VSD is positively charged and these charges move in response to voltage changes. In the resting state S4 is pulled inwards resulting in a closed channel. After depolarization however the S4 helices move outwards, causing conformational changes leading to channel opening (Fernández-Quintero et al. 2021).

Depending on the Cav2.x channel, Gβγ can bind at the N-terminus, I-II loop (linker between domain 1 and domain 2) and or C-terminus with different affinities according to experimental data. Although VSD1 is not a direct binding site, Gβγ mainly inhibits VSD I by stabilizing its reluctant state, reducing opening probability and slowing activation kinetics. It also inhibits VSD IV to a modest degree but when VSD I is inhibited, the other VSDs are not enough to support efficient pore opening by themselves (Nilsson et al. 2024).

Since the α subunit is the pore forming subunit, the selectivity filter is also included. It is formed by 4 glutamates in the pore: E314, E663, E1365 and E1655. These glutamates are located in the linkers between S5 and S6, at one of the most narrow segments of the pore (Dong et al. 2021).

The selectivity filter of calcium channels is a narrow region lined with negatively charged amino acids (mostly glutamates). These negative charges attract Ca^{2+} ions and coordinate them together with water molecules inside the pore. Because of this arrangement, Ca^{2+} ions can bind within the filter in multiple positions at the same time. When a new Ca^{2+} ion enters, it shifts the electrical and hydration balance in the filter. This change makes the previously bound ion move forward, allowing ions to pass through in a coordinated, stepwise "knock-on" process. The filter is flexible, so ion coordination and movement happen dynamically. Selectivity arises because Ca^{2+} interacts strongly and stably with this negatively charged environment, while Na^{+} and K^{+} cannot stabilize these interactions as effectively (Zhu et al. 2023; Yao et al. 2024).

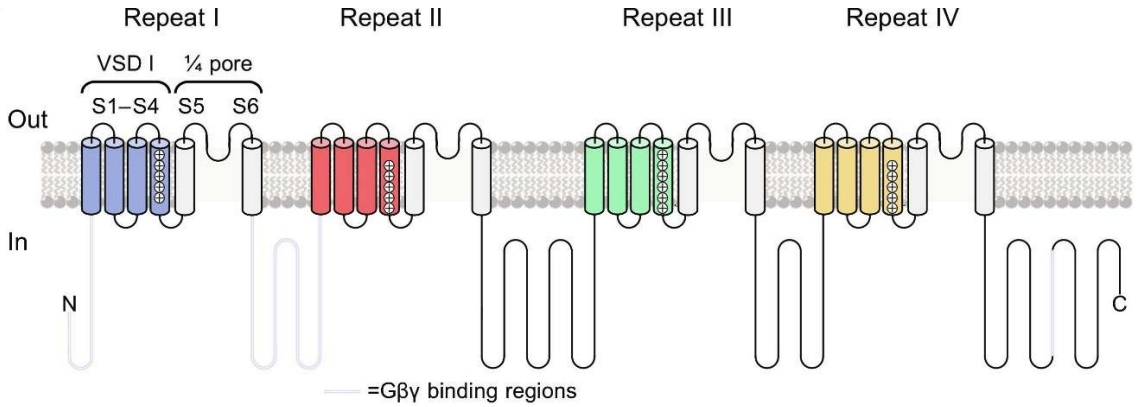

Figure 7 Cavα

(Nilsson et al. 2024)

1.3.2 Cav2.x β subunit (CACBx)

There are different types of Cav2.x β subunits: β1, β2, β3 and β4 with various subtypes like β2a, β2b, etc (Mayo et al. 2023).

CACBx consists of 5 regions (Fig. 8):

- N-terminus
- C-terminus
- SH3 domain (Src homology 3 domain 3)
- GK domain (guanylate kinase domain)
- HOOK that connects SH3 and GK (Park and Suh 2018)

GK is catalytically inactive and binds tightly to the AID (α-Interaction Domain), the 18 amino acid long binding site for Cavβ in Cavα. SH3 is made of 5 β strands (βstrand 1–5) with the last 2 divided by the HOOK region. The HOOK region and the termini can vary in different β subunit isoforms. The HOOK region is likely highly flexible and a protagonist in channel inactivation. Intramolecular interaction

between GK and SH3 is possible and plays a role in CACBx ability to modulate channel gating, which was proven by mutations that hindered this interaction (Buraei and Yang 2010).

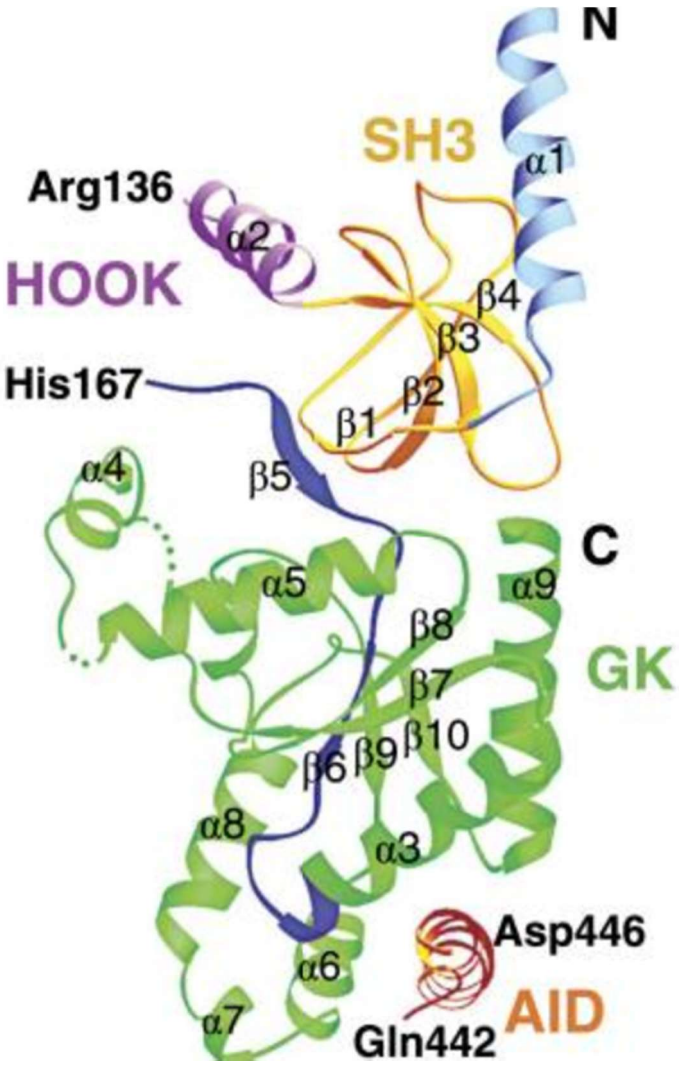

Figure 8 β3 regions

(Buraei and Yang 2010)

The β subunit is an auxillary subunit responsible for gating of Cav2.x channels. The N-terminus of certain subtypes is capable of binding the membrane while the β subunit is also bound to the α subunit. When Cav2.2 is expressed with cytosolic isoforms β2b and β3 that are not bound to the membrane, it exhibits fast current inactivation, high sensitivity to depletion of PIP2 and low current density. When expressed with isoforms β2a and β2e that bind both the α subunit and the membrane, it exhibits slow current inactivation, low sensitivity to depletion of PIP2 and high current density (Fig. 9). Opposite results were achieved with the sole difference of membrane binding, ergo the isoform of the β subunit drastically impacts the modulation of Cav2.x channel gating (Park and Suh 2018).

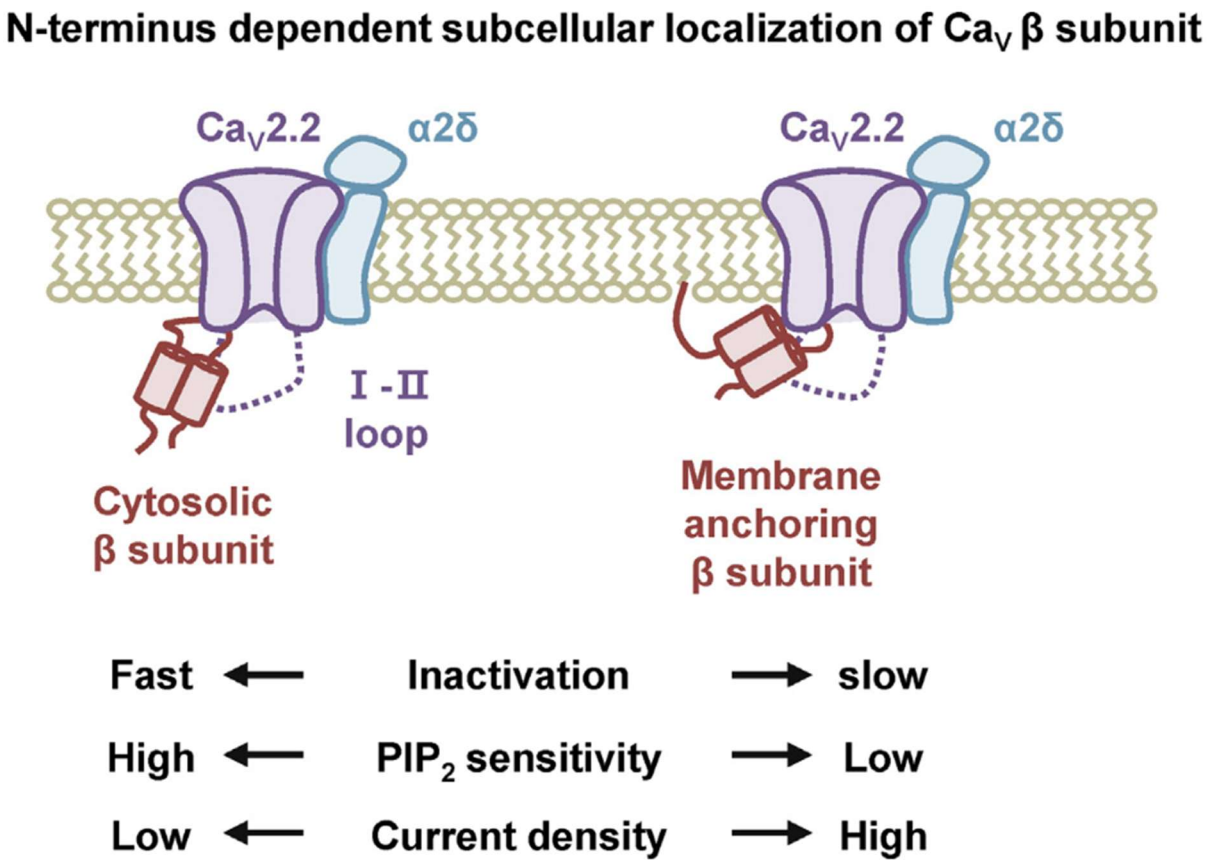

Figure 9 Cytosolic vs membrane anchoring β subunit

(Park and Suh 2018)

Cav2.x channel gating can also be affected by the net surface charge of the HOOK region. The net surface charge affects the HOOK regions ability to interact electrostatically with the membrane. In Cav2.2 an acidic HOOK region accelerates current inactivation, increases PIP2 sensitivity and decreases current density. A basic Hook region on the other hand slows current inactivation, reduces PIP2 sensitivity and increases current density (Fig. 10). These are opposite effects, ergo HOOK mediated membrane interaction drastically effects Cav2.x channel gating, just like the β subunit isoform does (Park and Suh 2018).

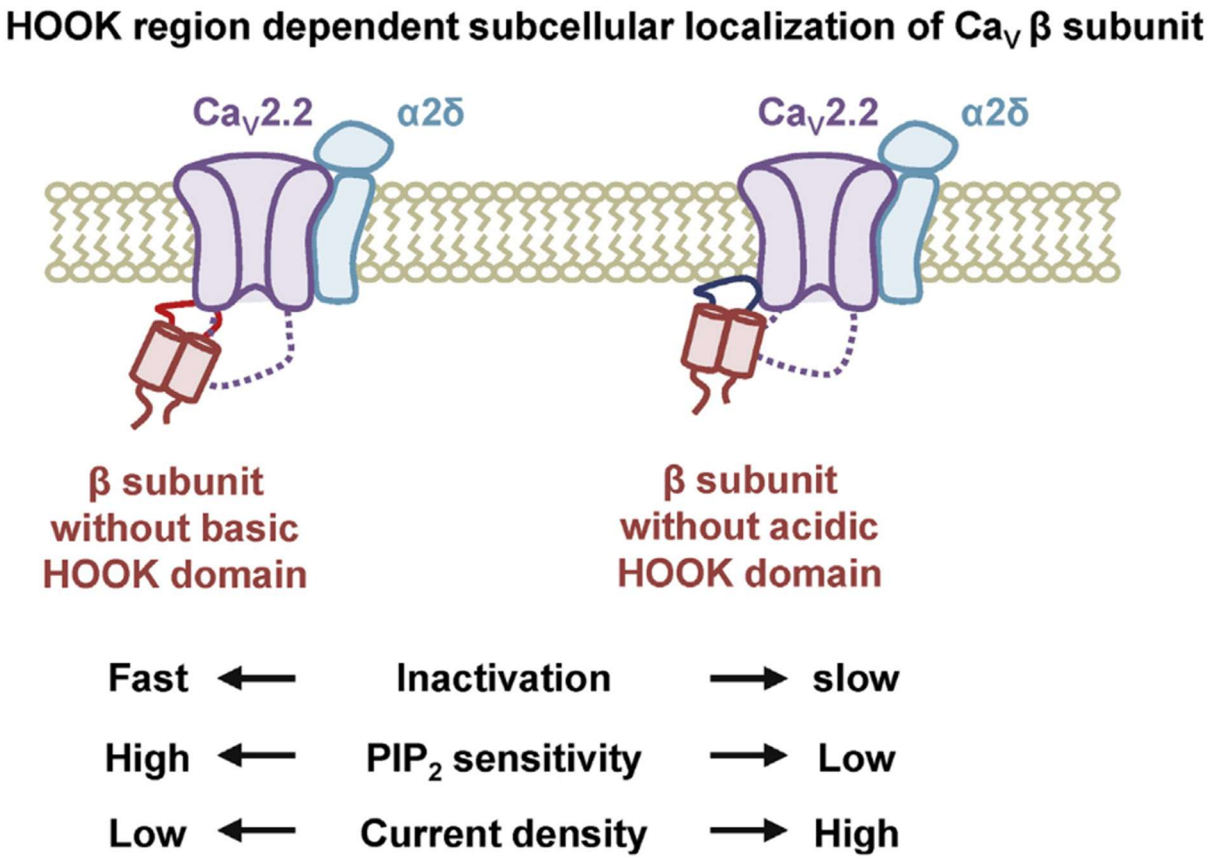

Figure 10 Acidic vs basic HOOK region

(Park and Suh 2018)

The β subunit functions as a chaperone for Cav1.x and Cav2.x channels, mostly via its GK domain and membrane-tethered β subunits can increase membrane Cav2.x expression. Therefore the β subunit regulates membrane expression of Cav2.x channels via channel expression in general and localization to the membrane (Buraei and Yang 2010).

1.3.2.1 CACNA1x-CACBx-binding

The α and β subunit of Cav2.x bind in order to form the channel. The alpha interaction domain (AID) of CACNA1x binds the AID-binding pocket (ABP) in the GK domain of CACBx. The AID is an 18 residue (QQxExxLxGYxxWIxxxE) long stretch that is present in the I-II loop of the α subunit of all Cav1.x and Cav2.x channels. It is able to bind all 4 β subunits and their isoforms. Point mutations of AID residues Y10, W13, and I14 have been proven to drastically reduce interaction with the β subunit. CACBx contains a 31 residue long beta interaction domain (BID) that does not directly bind CACNA1x, although 4 BID point mutations were found to affect binding of the α subunit. 3 of these 4 point mutations are either proline or tyrosine and likely affected the folding ability of Cavβ and SH3-GK intramolecular interaction, resulting in abolished α subunit binding (Buraei and Yang 2010).

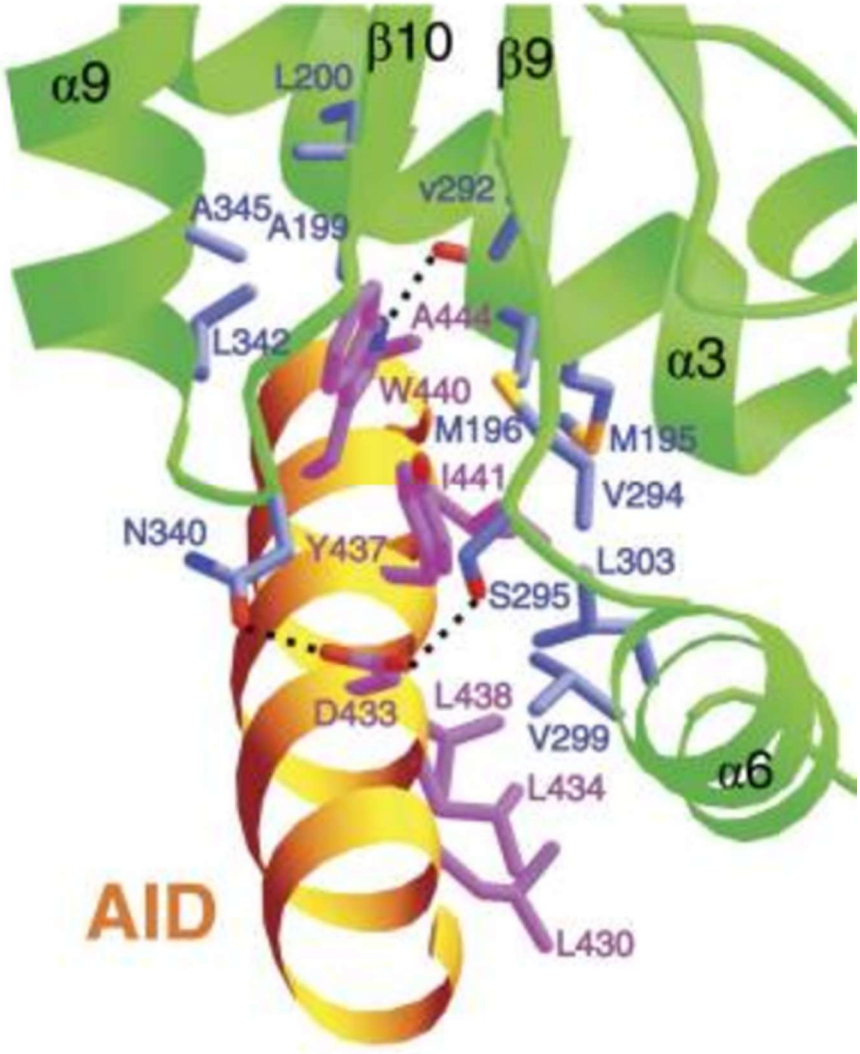

Figure 11 AID-β3 interaction

Text (Buraei and Yang 2010)

1.3.2.2 Relevance of β subunit in Gβγ mediated inhibition

As mentioned in chapter 1.2.2 inhibition via Gβγ binding of CACNA1x can be eliminated by voltage. However this observation cannot be made in channels that do not contain the β subunit. CACNA1B point mutation W391A in tsA-201 cells is an AID variant that is unable to bind the β subunit and does not display voltage dependent inhibition via Gβγ. M245A and L249A in β2a of Xenopuss Oocytes cause a loss of the ability to bind CACNA1A and also abolish voltage dependent inhibition via Gβγ. The aforementioned variants can still be inhibited by Gβγ independently from voltage, but the ability to reverse inhibition with voltage is lost. These findings suggest that the β subunit is necessary for the voltage dependent dissociation of Gβγ in inhibited Cav2.x channels. The strength of voltage dependent inhibition depends on the type of β subunit because the different types promote dissociation of Gβγ

to different extents (β3 > β2 > β1b > β2a). The GK domain of Cavβ by itself is sufficient for this process in Cav2.1 and Cav2.2 (Buraei and Yang 2010).

Many binding partners of Gβγ contain the QxxER sequence as a binding site, which also happen to be the first 5 residues of the AID (QQIER in Cav2.1, Cav2.2 and Cav2.3) (Zamponi and Currie 2013).

This information could lead to the conclusion that Gβγ and Cavβ compete for binding of the AID. However we do know that the β subunit is responsible for voltage dependent dissociation of Gβγ in inhibited Cav2.x channels, indicating that both are bound to the α subunit. Both voltage dependent inhibition (VDI) and voltage dependent activation (VDA) remain unchanged before, during and after modulation, further indicating that Cavβ remains bound to Cavα during Gβγ inhibition (Buraei and Yang 2010).

An explanation for this could be that Cavβ partially dissociates in order to allow Gβγ binding, or that Gβγ only binds the residues of the AID that are not taken by Cavβ (Zamponi and Currie 2013).

Inserting 3-7 glycines into the linker between α-helix S6 of Domain I and the AID abolishes Cavβ modulation of Cav2.x channel gating and therefore also abolishes VDI via Gβγ (Fig 12C). Binding of Gβγ however stays intact and therefore so does voltage independent inhibition. Inserting 5 alanines in Cav2.1 however abolishes both voltage dependent and voltage independent inhibition, probably due to causing a 180 degree turn of the β-helix, potentially causing an inability to bind Cavβ. Hence a rigid IS6-AID linker seems to be essential for VDI (Buraei and Yang 2010).

1.3.2.3 Gβγ inhibition model by Buraei and Yang

Buraei and Yang proposed that he I-II loop and the N-terminus form a GBP (Gβγ-binding-pocket). According to their model the I-II loop has 2 binding sites for Gβγ:

1. The QxxER motif and the residues upstream of it (Gβγ affinity ~60 nM)
2. Another one further downstream in the AID (Gβγ affinity ~20 nM)

When Cavβ is bound to the AID the upstream QxxER containing binding site is partially buried, meaning that Gβγ binding to the upstream binding site is drastically weaker when Cavβ is present.

When Cavβ is bound to the AID, the IS6-AID linker and the AID form a continuous α-helix that mechanically couples the pore domain to the I-II loop. Buraei and Yang proposed that movement of the S6 helices during strong depolarization (pore opening) is transmitted through the α-helical IS6-AID linker to the I-II loop, destabilizing interactions between Gβγ and the Cav2.x channel and therefore contributing to voltage-dependent relief of inhibition (Fig. 12A) In the absence of CaVβ voltage-dependent relief of inhibition is largely lost, consistent with the idea that the α-helical coupling mechanism is disrupted, explaining why voltage does not dissociate Gβγ in β-less channels (Fig 12B).

As mentioned in chapter 1.3.2.2, the insertion of 3-7 glycines abolishes Cavβ modulation of Cav2.x channel gating and therefore also abolishes VDI via Gβγ. This insertion seems to disrupt the α-helical

continuity of the IS6-AID region and therefore impairs conformational coupling between the pore domain and the I-II loop, preventing voltage dependent dissociation of Gβγ (Fig 12C) (Buraei and Yang 2010).

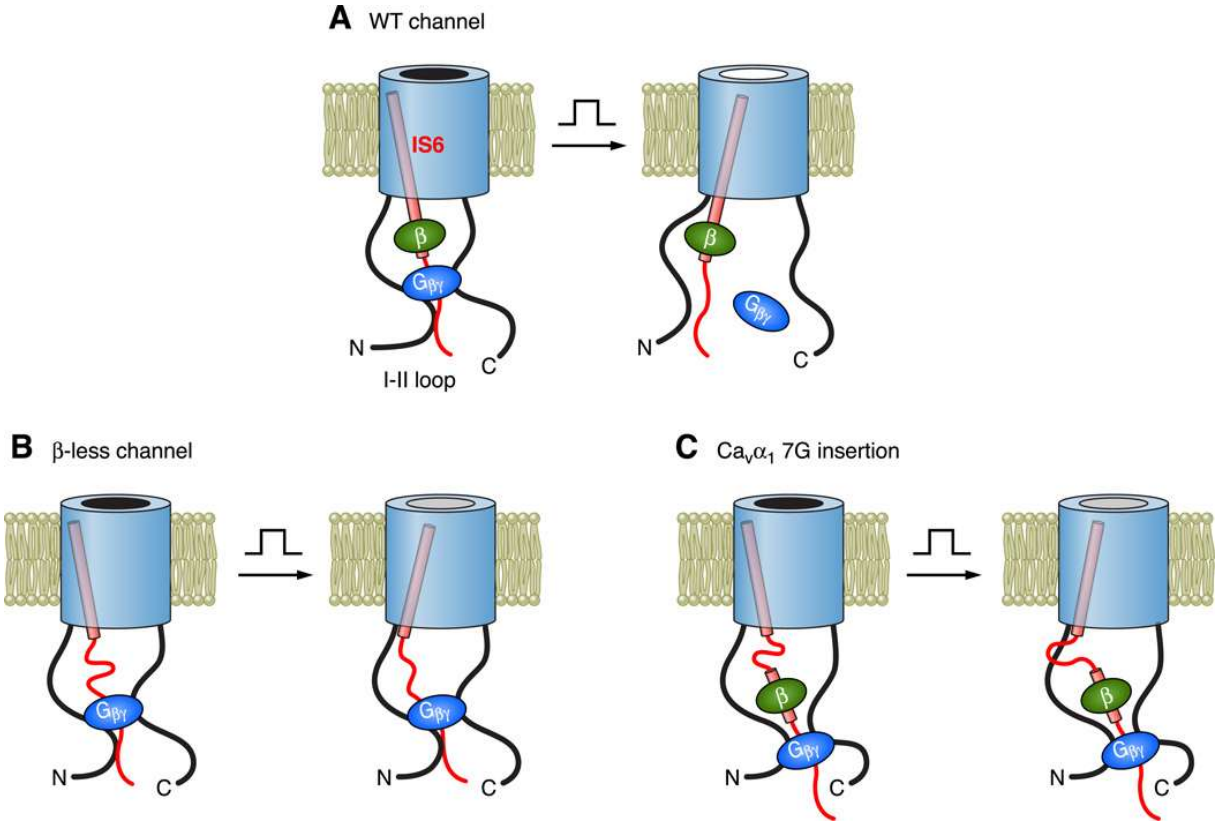

Figure 12 Gβγ inhibition model by Buraei and Yang

(A) In the wild type channel the I-II loop and N-terminus form a Gβγ-gated inhibitory module and the inhibition is voltage dependent

(B) Channels without Cavβ are inhibited independently from voltage since Gβγ binding is much stronger in the absence of Cavβ

(C) Inserting 7 glycines into the IS6-AID linker disrupts the α-helix, uncoupling IS6 from the GBP and abolishing voltage-dependent dissociation of Gβγ (Buraei and Yang 2010)

There is supporting evidence of this GBP formation theory. Mutations in both the N-terminus and the I-II loop affect Gβγ mediated inhibition (Tedford et al. 2010), but kinetic data supports 1:1 stoichiometry, inferring that both the N-terminus and the I-II loop interact with Gβγ at the same time (Lacinova et al. 2020).

Sidenote: The I-II loop and the N-terminus forming the GBP is not shown in the AlphaFold predictions, however the idea of a mobile I-II loop is supported multiple times in this thesis. The AlphaFold

prediction also predicts a continuous α-helix containing the IS6-AID linker and the AID in the absence Gβγ with good confidence.

1.3.3 Cav2.x α2δ subunit

The α2δ subunit is located extracellularly, binding Cavα via interacting with multiple extracellular loops of Cavα (Gurnett et al. 1997). The δ region of α2δ is tethered to the membrane via a glycosylphosphatidylinositol (GPI) anchor, but it's not a transmembrane segment (Davies et al. 2010). The α2δ(1-4) subunit is an auxiliary subunit that increases Cavα transport to the membrane and its retention there, hence increasing Ca2+ flow. It is also linked to regulation of synaptogenesis as a receptor for thrombospondin. The α2δ1 subtype can be targeted pharmacologically in treatment of epilepsy and neuropathic pain (Buraei and Yang 2010).

Expressing $\alpha_2\delta1$ with $Ca_V2.2/\beta1b$ resulted in shorter channel open times and multiple studies indicate that the α2δ subunit increases Cav2.x inactivation. Effects on Cav2.x channel voltage dependence vary when α2δ is combined with a multitude of other Cav subunits, especially with different Cavα subunits (Dolphin 2013).

1.3.4 Cav2.x γ subunit

In cryo-EM this subunit sits within the membrane environment and interacts with Cavα α-helices via lipid-exposed transmembrane surfaces (Zamponi 2017).

The γ(1-8) subunits seem to vary in function with γ2-4 and γ8 primarily being AMPA (α-amino-3-hydroxy-5-methyl-4-isoxazole propionic acid) receptor regulatory proteins (TARPs). The γ subunit of Cav2.x channels contains 4 transmembrane segments and intracellular N- and C-termini (Buraei and Yang 2010).

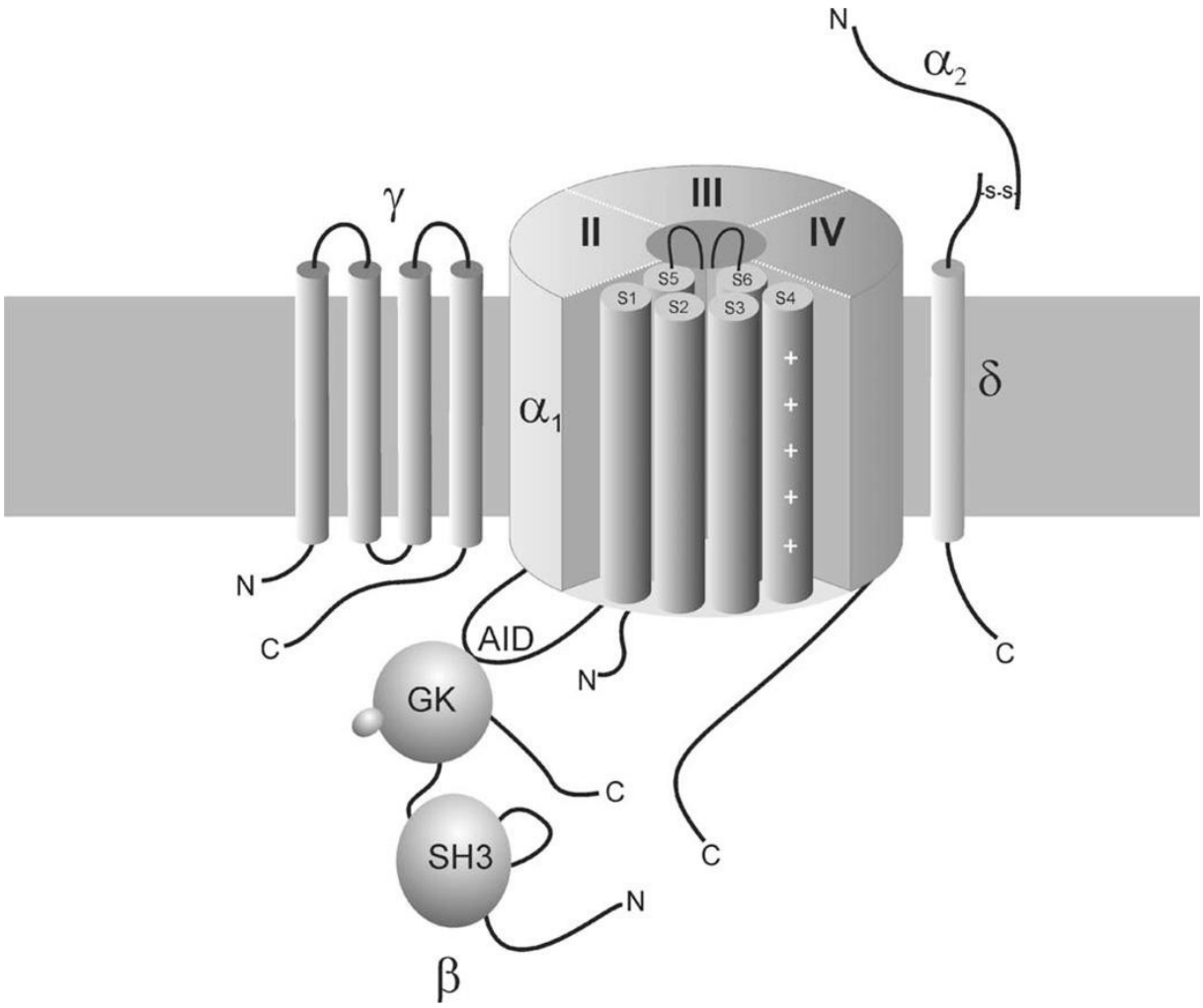

Figure 13 Cav2 channel with all subunits (Jeziorski and Greenberg 2006)

1.3.5 Calmodulin

Calmodulin (CaM) is encoded by three genes (CALM1–3), all of which produce an identical mature protein. In Cav2 channels, CaM is constitutively preassociated with the C-terminal regulatory region, primarily through the IQ domain, where it functions as an intrinsic Ca2+ sensor. Upon Ca2+ binding, CaM mediates Ca2+-dependent regulation of channel activity, including facilitation and/or inactivation (DeMaria et al. 2001; Pang et al. 2010; Ben-Johny and Yue 2014)

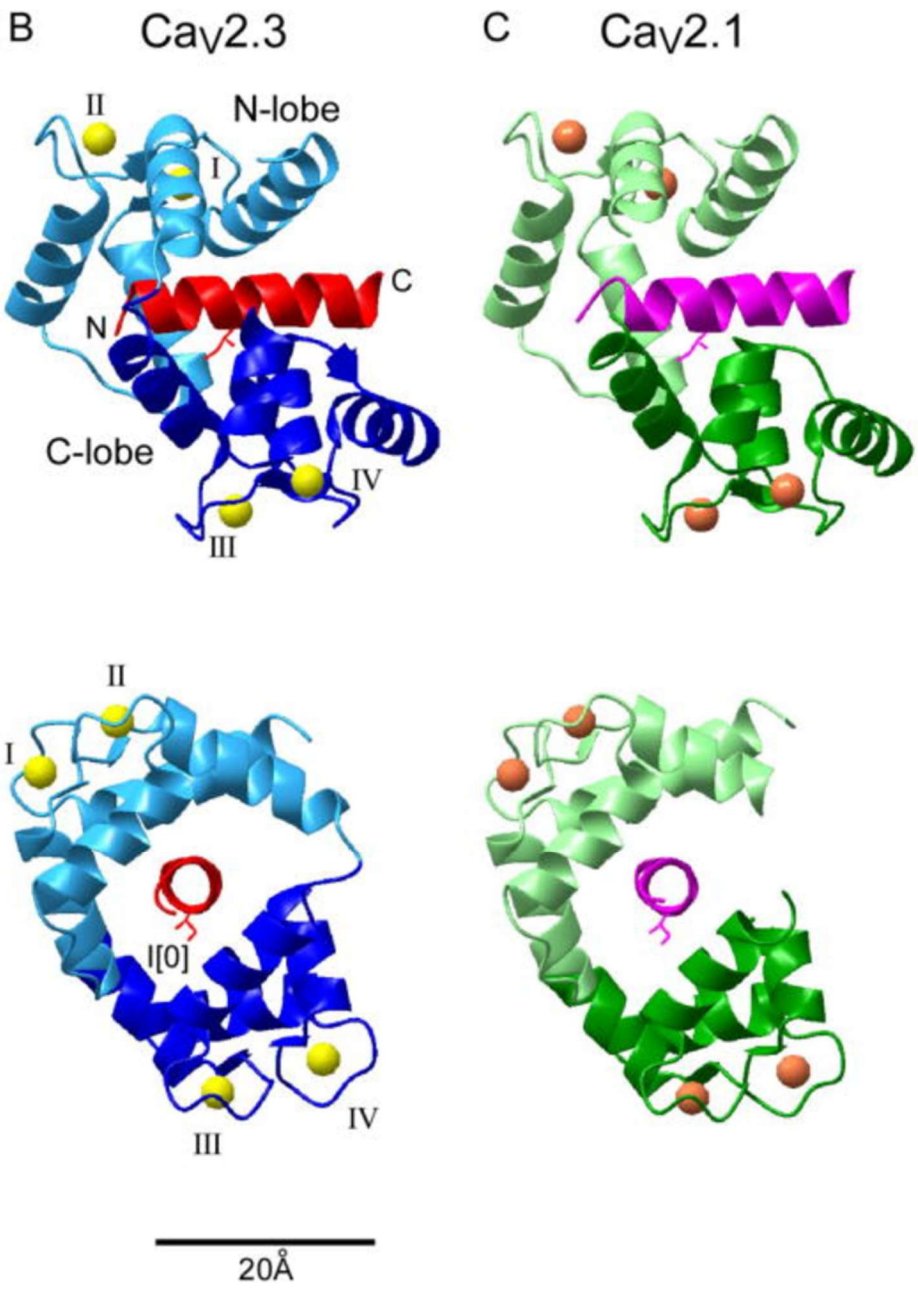

Figure 14 Calmodulin binding to the IQ-motif

IQ-motif is red/magenta, N-lobe and C-lobe of CaM are different shades of blue/green, calcium ions are yellow (Mori et al. 2008)

1.3.6 Function without α2δ and γ subunits

Channel function (rat-Cav2.2/β3 in HEK-293 cells) persists when α2δ and γ subunits are not expressed. Current activation and inactivation speed are reduced when α2δ subunit is removed, but function is not abolished (Fig. 15) (Andrade et al. 2007).

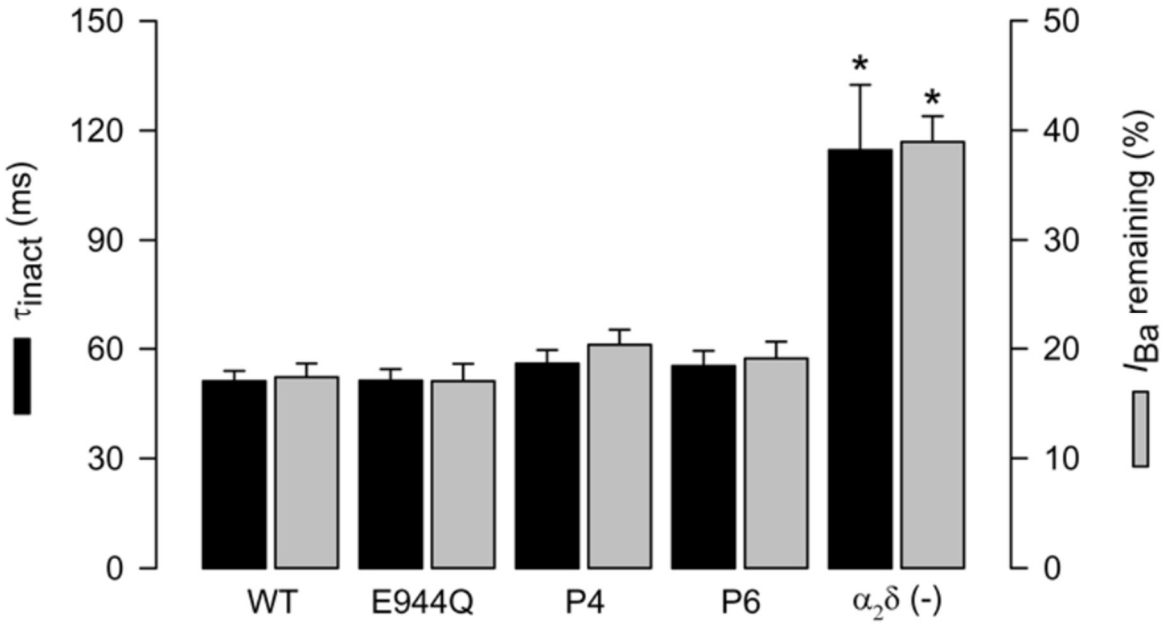

Figure 15 Function with and without α2δ subunits

(Andrade et al. 2007)

The α2δ and γ subunits are not located at neither the N- or C-terminus of Cavα nor the AID (Fig. 13). Therefore they are not in the Gβ1γ2 binding region.

1.4 Subunit combinations used in this thesis

As mentioned in chapter 1.3.2.1 the α subunit of Cav2.x channels contains the AID, where the β subunit binds. This concerns every subtype of Cavβ, meaning that every Cavβ subunit can bind the α subunit of Cav2.x channels. (Buraei and Yang 2010)

In Mice Cav2.1 and Cavβ4 are both highly expressed in the cerebellar neurons, creating a high likelihood of association. Furthermore β4 knockout mice showed substantially reduced high-voltage-activated Ca^{2+} currents and abnormal excitability of the central nervous system, which can also occur in GNB1-E. This could be linked to the cerebellum, therefore this thesis simulates Cav2.1 with Cavβ4. (Catterall 2011; Vendel et al. 2006; Burgess et al., n.d.)

Cav2.2 is expressed with Cavβ3 in this thesis due to Cavβ3's preference in mice to associate with Cav2.2 in sympathetic neurons according to Murakami, therefore increasing Cav2.2 expression. This indicates a likelihood that a majority of sympathetic Cav2.2 channels are associated with Cavβ3. Furthermore an experiment in transgenic mice that overexpress Cavβ3 resulted in increased sympathetic Cav2.2 expression and therefore function, specifically in supracervical ganglion neurons. (Murakami et al. 2008)

CaV2.3 and β3 both show regional expression in the human cortex and hippocampus, meaning that association in these regions is likely. Therefore this thesis combines them in its simulations. (Hawrylycz et al. 2012; Kjær et al. 2023)

2 Objective

GNB1-E is a disease caused by mutations in the Gβ subunit. Since the Gβγ dimer inhibits Cav2.x channels intracellularly, these mutations can affect channel function. Currently cryo-EM structures of Cav2.x channels are only available for the transmembrane segment, not the entire channel. Therefore AlphaFold simulations could add value since the program folds the entire protein and not just the transmembrane part.

This thesis compares currently known structural information of Cav2.1, Cav2.2 and Cav2.3 to the structures predicted by AlphaFold in order to determine whether or not the AlphaFold predictions can be used for further simulations. Furthermore the predicted binding position of Gβ1γ2 on the different Cav2.x channels is assessed based on currently available experimental data.

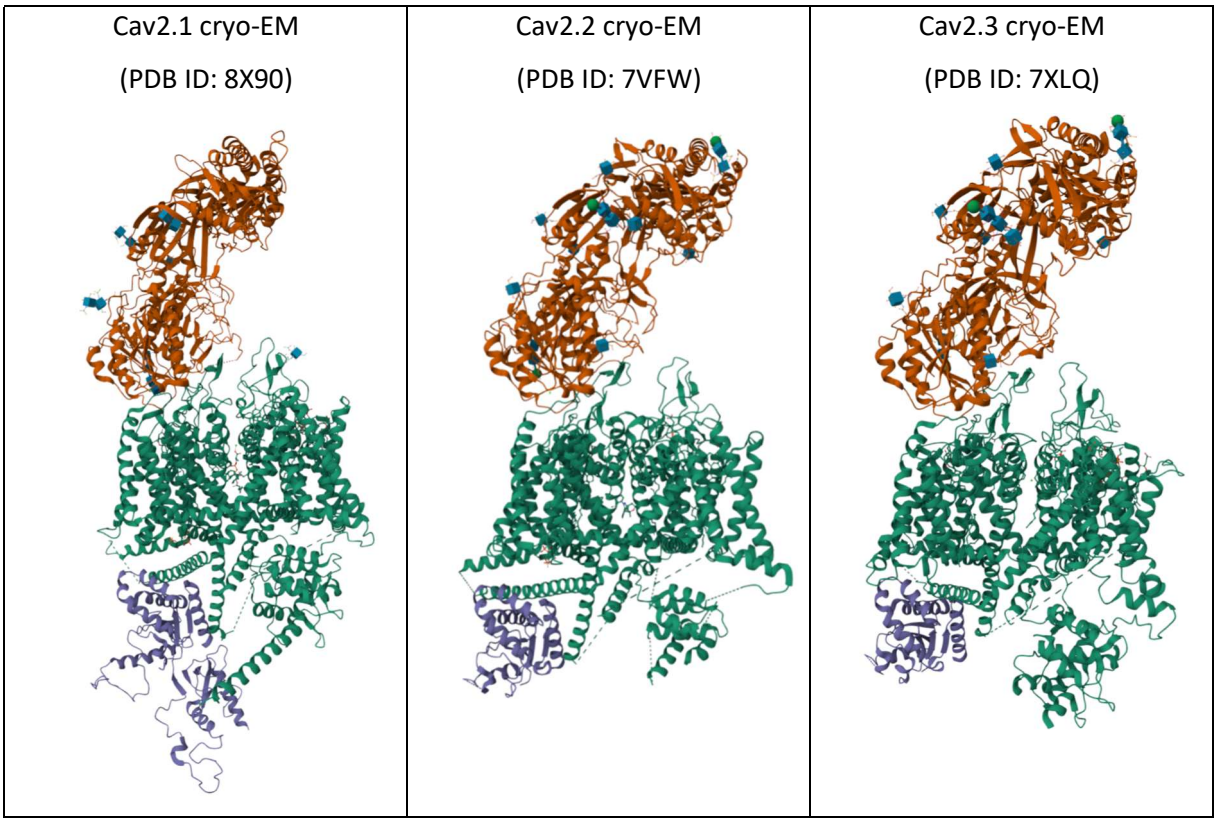

Figure 16 Cryo-EM structures from https://www.rcsb.org/

Channel	PDB ID	Subunits
Cav2.1	8X90	CACNA1A CACNA2D1 CACNB3
Cav2.2	7VFW	CACNA1B CACNA2D1 CACNB1
	7MIY	CACNA1B CACNA2D1 CACNB3
	7MIX	CACNA1B CACNA2D1 CACNB3
	7VFS	CACNA1B CACNA2D1 CACNB1
	7VFV	CACNA1B CACNA2D1 CACNB1
	7VFU	CACNA1B CACNA2D1 CACNB1
Cav2.3	should be 7XLQ	CACNA1E CACNA2D1 CACNB1

Table 1 PDB data

3 Materials and Methods

3.1 Software

The protein folding simulations were carried out with AlphaFold, an artificial intelligence program that folds amino acid sequences into 3D protein structures, accessible on alphafoldserver.com.

AlphaFold uses neural-network architectures trained on large datasets of experimentally determined molecular structures to infer the three-dimensional arrangement of atoms directly from sequence information. It predicts biomolecular structures by learning statistical patterns from experimentally determined structures and sequence data. It integrates evolutionary relationships derived from multiple-sequence alignments with attention-based neural networks that model spatial relationships between residues and iteratively optimize atomic arrangements. The system can also generate structural predictions for complexes containing proteins, nucleic acids, ligands, and ions through diffusion-based modeling approaches that estimate the most probable interaction geometries and conformations (Abramson et al. 2024; Jumper et al. 2021).

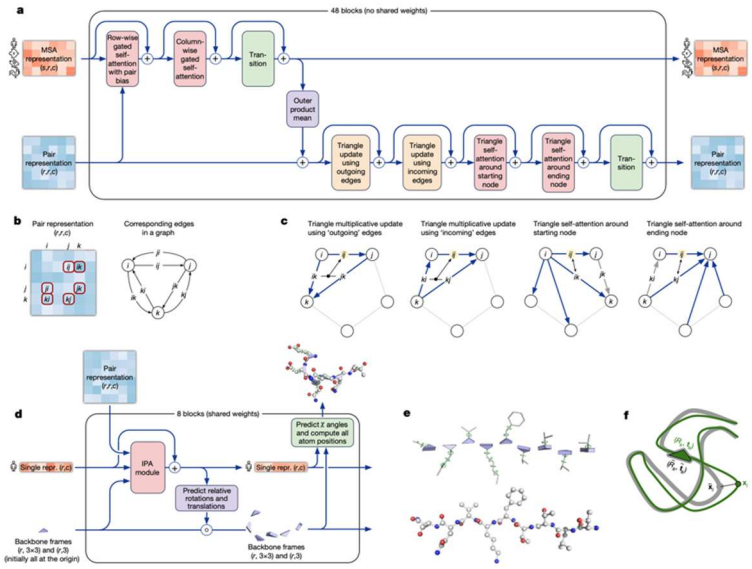

Figure 17

The main metrics according to alphafoldserver.com are:

- **pLDDT** (predicted local distance difference test)**:** Confidence per atom on a spectrum of 0-100 visualized by a colour code. The colours visualize how likely accurate the 3D structure of the coloured residue is predicated in formation and location. Dark blue residues resemble very high confidence (>90), cyan residues resemble good confidence (70<x<90), yellow resembles low confidence (50<x<70) and orange resembles very low confidence (<50)
- **pTM** (predicted template modelling score): An overall confidence score on a spectrum of 0-1, that predicts how likely accurate the predicted proteins are overall. Therefore a prediction with a score of <0,5 is likely inaccurate and a prediction with a score of >0,5 is more likely accurate than not or at least similar enough.
- **ipTM** (interface predicted template modelling score): This confidence score is relevant for predictions that include multiple proteins. It shows how likely accurate the positioning of the different proteins is, which is important for predicting the interacting interfaces. Like pTM it's also on a spectrum of 0-1 but the scores are valued differently. Score >0,8 are viewed as likely accurate and scores <0,6 are viewed as likely failed predictions
- **PAE** (predicted aligned error): A confidence metric to estimate how accurately the relative positions of different regions in a predicted structure are modeled. Specifically, it predicts the expected positional error in Ångströms for one residue when the model is aligned on another residue. Low PAE values indicate high confidence in the relative orientation between regions, whereas high PAE values suggest uncertainty or flexibility in their spatial arrangement. PAE is

particularly useful for evaluating domain orientations and protein–protein interaction interfaces in predicted complexes.

- **Fraction disordered**: Describes the proportion of residues in a predicted protein structure that are expected to lack a stable, well defined 3D conformation. A higher fraction disordered value suggests that larger regions of the protein are likely to be flexible or intrinsically disordered rather than forming rigid secondary or tertiary structures.

Once entering a sequence into AlphaFold, the PDB template can be changed. In this thesis, the newest template available at the time was used: febuary 3rd 2025.

3.2 Amino acid sequence sources

The different amino acid sequences for the different Cav2.x channel subunits, different calmodulins and Gβγ were taken from UniProt [https://www.uniprot.org], an online protein sequence database. The following human UniProt sequences were used:

- Gβ1 (GNB1): P62873
- Gγ2 (GNG2): P59768
- Cav2.1 α subunit (CACNA1A): O00555
- Cav2.2 α subunit (CACNA1B): Q00975
- Cav2.3 α subunit (CACNA1E): Q15878
- CALM1: P0DP23
- CALM2: P0DP24
- CALM3: P0DP25
- Cavβ3 (CACNB3): P54284
- Cavβ4 (CACNB4): O00305

3.3 Visualization

The structures given by AlphaFold were then visualized via PyMol in order to visually separate the different Cav2.x subunits, calmodulin and Gβ1 and Gγ2 by colouring them differently. PyMol was also used for rendering of the snapshots in order to creature pictures of higher quality.

4 Results and Discussion

4.1 AlphaFold (AF) predictions

Addition of the β, Gβ1γ2, and CaM subunits during joint modelling of Cav2.x protein complexes increased the folding quality of the α1 subunit (Figure 18A and Figures 19-21) and improved the accuracy of the Gβ1γ2 binding site prediction for Cav2.x channels. Notably, the Fraction Disordered metric decreased to values below 0.05 upon addition of either the β or Gβ1γ2 subunit alone. Further increases in complex composition did not result in additional improvement of this metric. In particular, the Fraction Disordered value remained below 0.05 for both the Gβ1γ2–Cav2.x α1/β and Gβ1γ2–Cav2.x α1/β–CaM complexes (Figure 18A).

Since Gβ1γ2 inhibits Cav2.x channels in the presence of the β subunit within the Cav2.x α1/β complex, this assembly represents the minimal functional complex for modelling Gβ1γ2 interactions with Cav2.x. The highest accuracy of α1–β interface prediction was achieved for the Gβ1γ2–Cav2.x α1/β complex and remained similar after addition of the CaM subunit. In these models, the α1–β interface was reproduced with a mean PAE of 15–25 Å and a minimum PAE of 1–2 Å, depending on the Cav2.x α1 isoform (Figure 18B).

Stepwise addition of the β and CaM subunits also improved prediction accuracy for the α1–Gβ1γ2 interface. In the Gβ1γ2–Cav2.x α1/β–CaM complex, this interface was predicted with a mean PAE of 15–20 Å and a minimum PAE of 1–2 Å, depending on the Cav2.x α1 subtype. Collectively, these results identify the Gβ1γ2–Cav2.x α1/β–CaM complex as the primary structural model used in this study (Figure 18C).

The interface PAE was calculated from the AlphaFold PAE matrix by selecting residue pairs whose heavy atoms were within 5 Å of each other. Because the AlphaFold PAE matrix is asymmetric, where $PAE(i,j)$ and $PAE\ (j,i)$ represent the expected positional error of different residues under different alignment references, a direction-independent interface confidence measure was obtained by symmetrizing the matrix. The resulting $PAE_{interface}(i,j)$ value represents the average predicted alignment error for the residue pair at the protein–protein interface. For each interface residue pair, the interface PAE was calculated as:

$$PAE_{interface}(i,j) = \frac{PAE(i,j) + PAE\ (j,i)}{2}$$

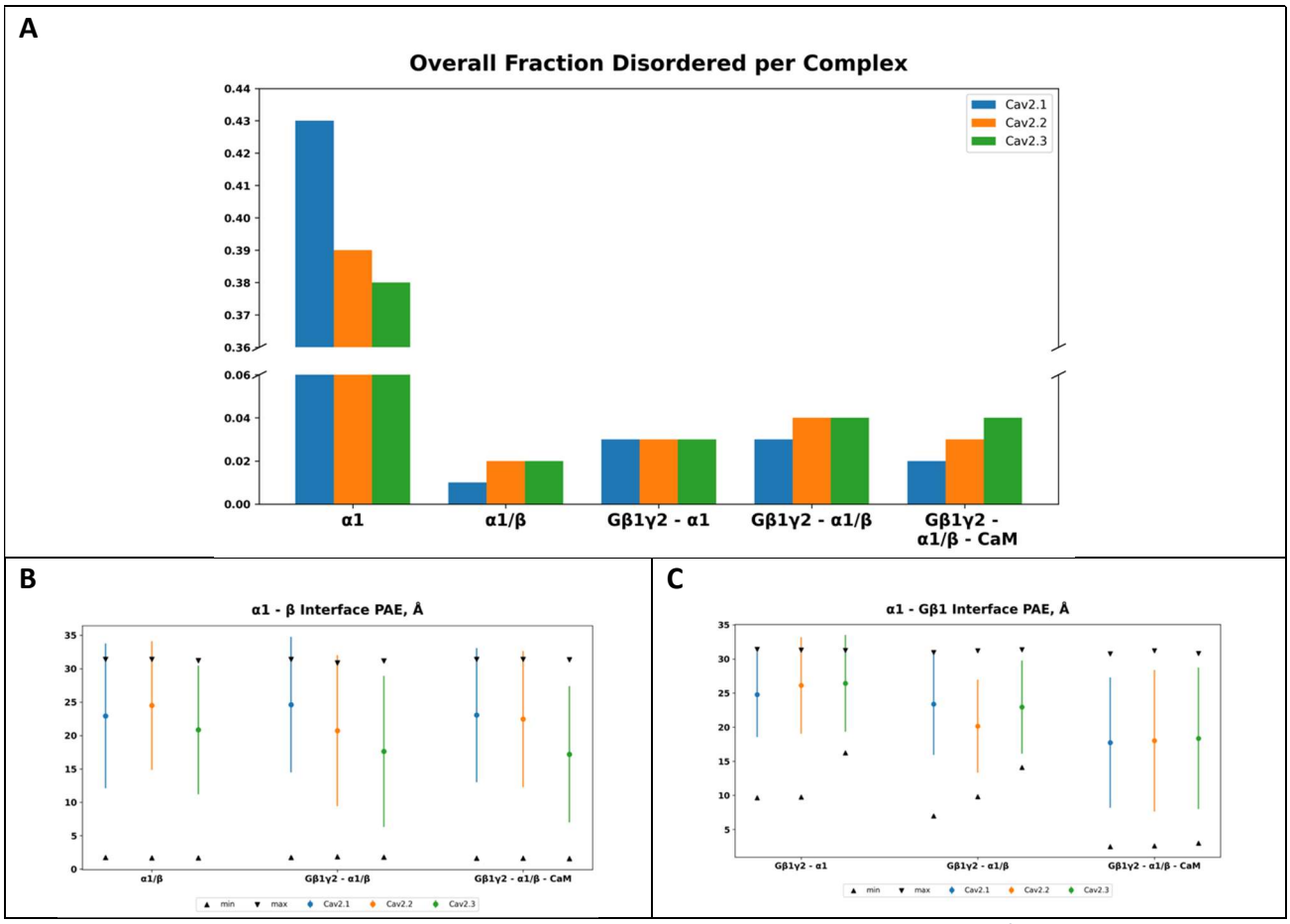

Figure 18 Changes in the fraction disordered of protein complexes and the PAE accuracy of Gb1g2/beta-alpha binding site prediction depending on the number of subunits

Figure 19. AlphaFold-Based Prediction of Cav2.1 Complexes

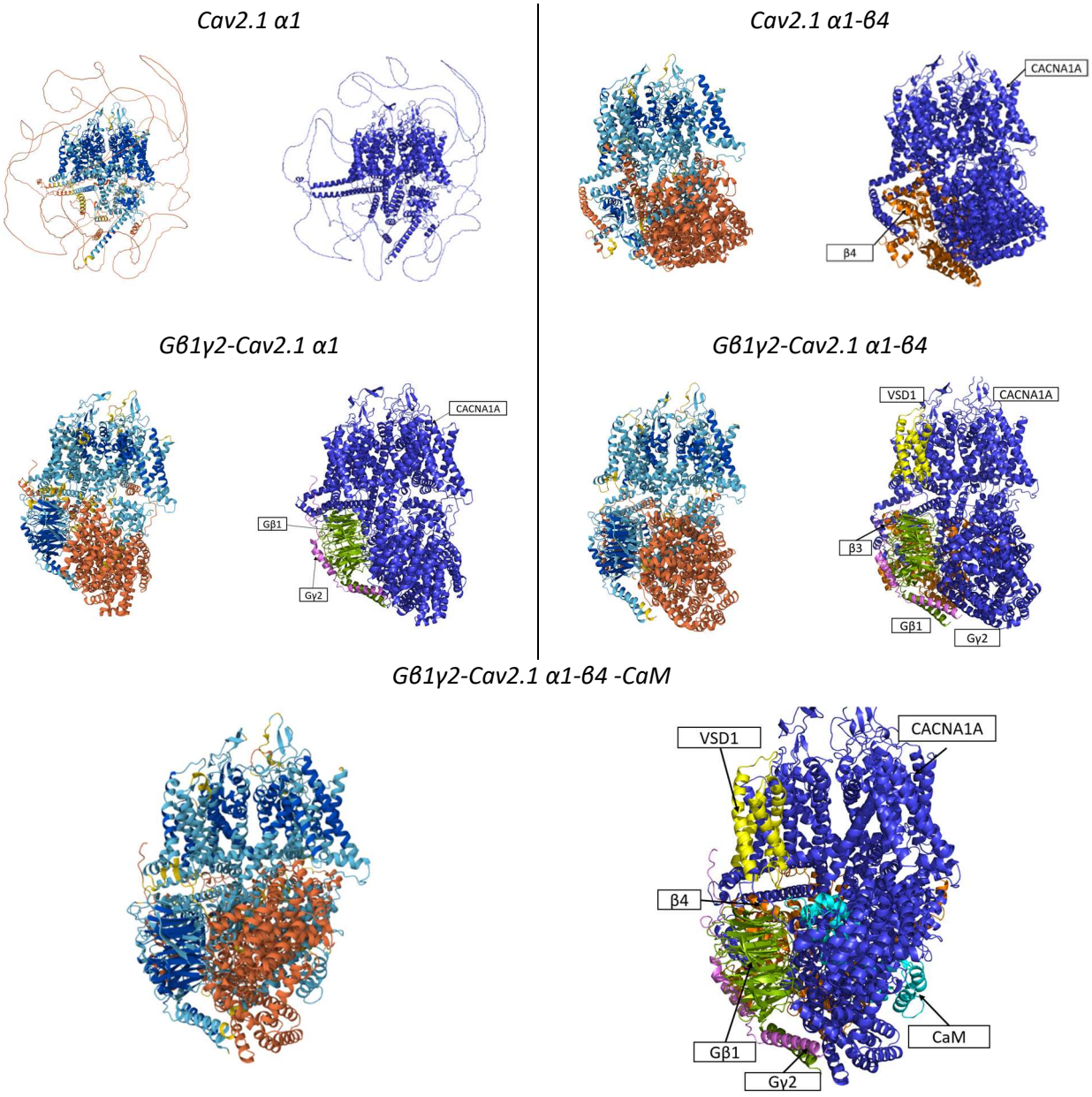

Figure 19 AlphaFold-Based Prediction of Cav2.1 Complexes

Figure 20. AlphaFold-Based Prediction of Cav2.2 Complexes

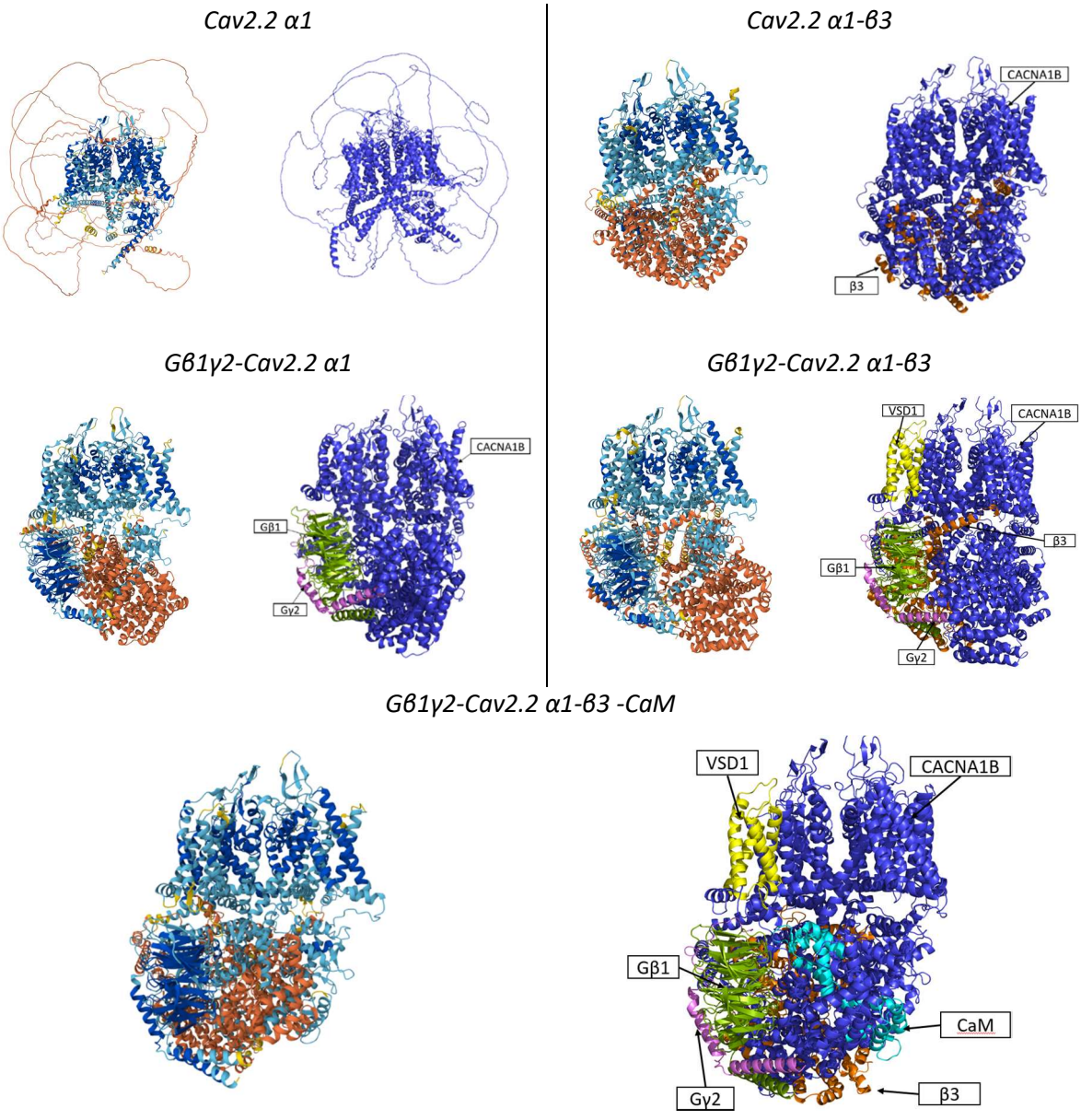

Figure 20 AlphaFold-Based Prediction of Cav2.2 Complexes

Figure 21. AlphaFold-Based Prediction of Cav2.3 Complexes

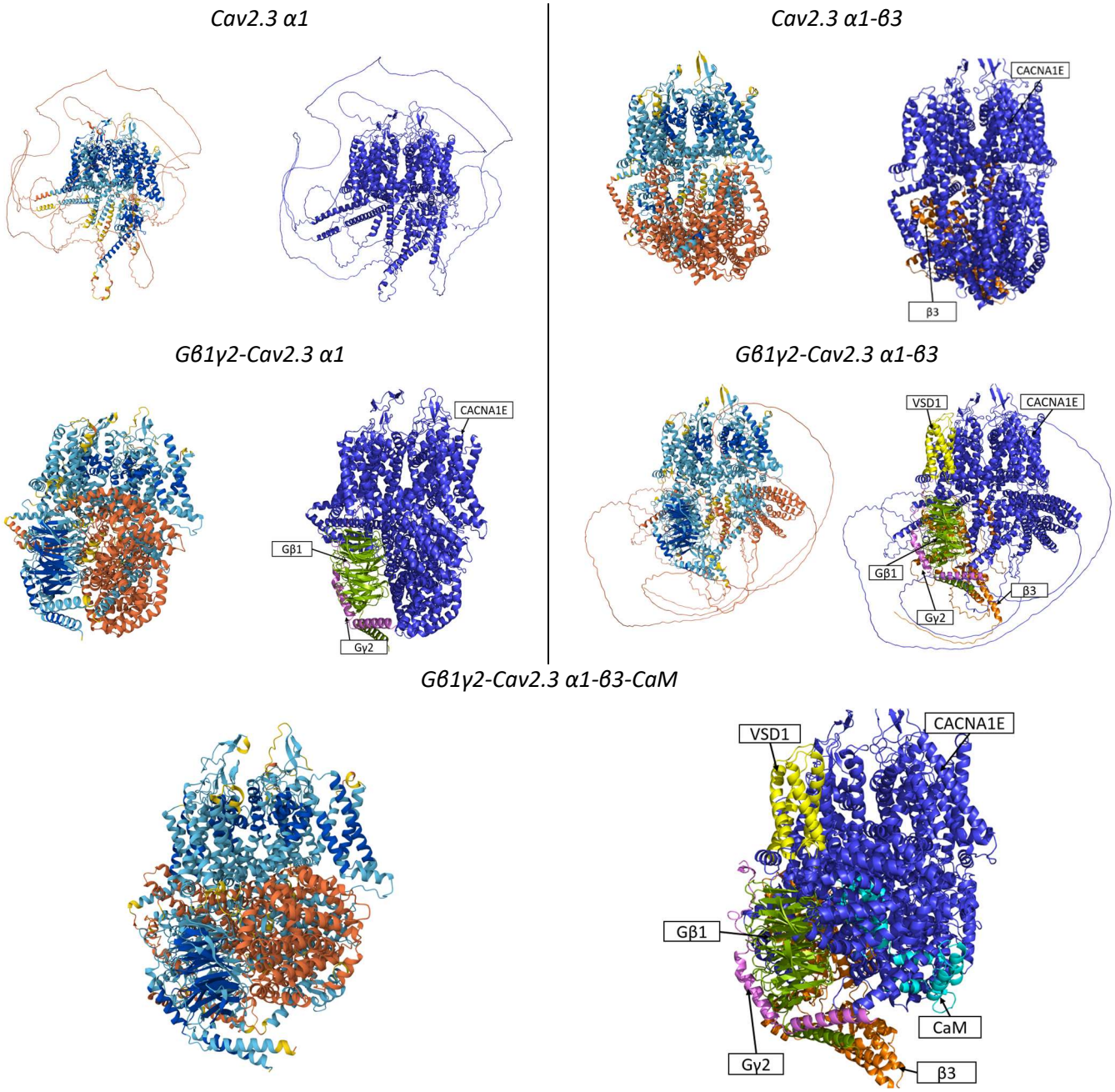

Figure 21 AlphaFold-Based Prediction of Cav2.3 Complexes

4.2 Comparison with experimental data

4.2.1 N-terminal binding

In every prediction above (Figs. 19-21) the Gβ1γ2 dimer is predicted to bind the N-terminal of Cavα and is located underneath VSD1. Experimental data of Cav2.2 supports the predicted binding site and identifies the interacting residues (Figs. 22A,B) (Cantí et al. 1999).

A

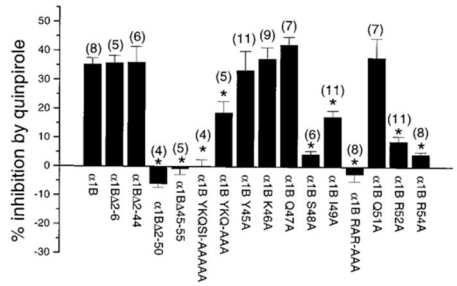

https://doi.org/10.1523/jneurosci.19-16-06855.1999

B

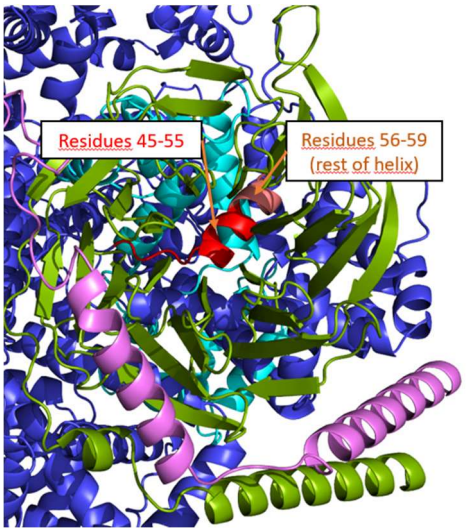

C

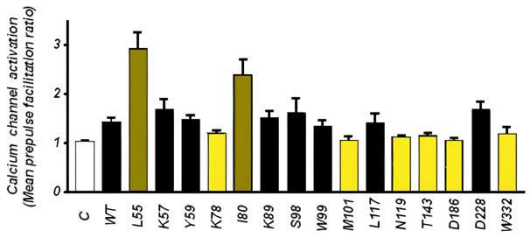

https://doi.org/10.1126/science.280.5367.1271

D

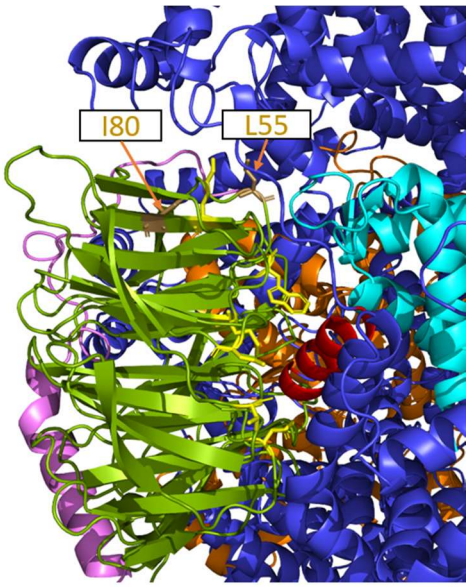

Figure 22 N-terminal Gβγ-Cav2.2α binding

Deleting residues 2-44 did not result in loss of inhibition, while deleting residues 2-50 did. Deleting residues 45-55 resulted in total loss of inhibition. Therefore residues 45-55 (YKQSIAQRART) were

identified as essential for modulation of CACNA1B by Gβ1γ2 (Fig. 22A). Afterwards point mutations in the aforementioned 11 amino acid stretch were made in order to identify the specific residues of the highest importance. This was achieved by mutating single residues to alanine. R52A and R54A showed complete loss of function, while S48A and I49A showed reduced inhibition, although I49A had a lesser effect than S48A. Mutating residues 45-47 to AAA also showed reduced modulation by Gβ1γ2, while mutating only one of them to alanine didn't significantly affect modulation by Gβ1γ2 (Cantí et al. 1999). The amino acid sequence YKQSIAQRART of the Cav2.2 α1 subunit is part of the binding site for the Gβ1γ2 subunit in the Gβ1γ2–Cav2.2 α1/β3–CaM complex predicted by AlphaFold (Figure 22B). Experimental data shows residues 45-55 (Fig. 22A) as essential for Gβ1γ2 mediated inhibition while AlphaFold predicts the α-helix at residues 49-59 as the binding site (Fig. 22B). According to the AlphaFold prediction residues 45-48 are therefore not the binding site but can effect binding according to Cantí.

Gβ1 residues involved in Gα binding were individually replaced with alanine, followed by assessment of their ability to inhibit Cav2.2α in HEK293 cells (Fig. 22C). The L55A and I80A mutations exhibited GoF effects, whereas the K78A, M101A, N119A, T143A, D186A, and W332A mutations caused LoF (Ford et al. 1998).

In the AlphaFold prediction (Fig. 22D) the aforementioned residues show proximity to the N-terminal α-helix (residues 49-59, Figure 19B), consistent with a role in Gβγ interaction for Cav2.2.

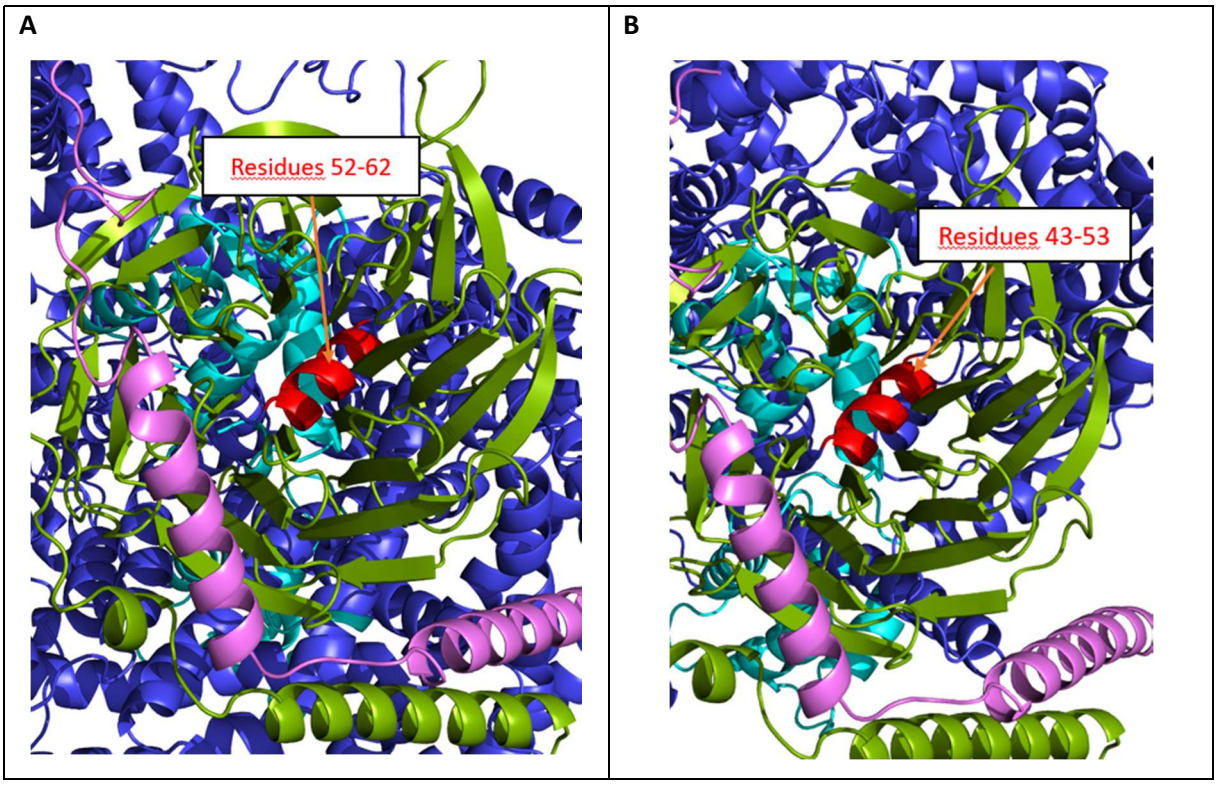

Figure 23 N-terminal Gβγ-binding α-helix in Cav2.1 and Cav2.3 predictions

An N-terminal 11 amino acid long α-helix in proximity to Gβ1γ2 can also be found in the AlphaFold predictions for Cav2.1 and Cav2.3 (Figs. 23A,B):

- Cav2.1 residues 52-62: M-A-Q-R-A-R-T-M-A-L-Y (Figure 23A)
- Cav2.2 residues 49-59: I-A-Q-R-A-R-T-M-A-L-Y (Figure 22B)
- Cav2.3: residues 43-53: K-A-Q-R-A-R-T-M-A-L-Y (Figure 23 B)

The helices differentiate in only the first amino acid and all show proximity to Gβ1γ2. Due to similar composition and position in relation to Gβ1γ2, the Gβ1γ2 mutations from figure 22C could potentially show similar effects on Cav2.1 and Cav2.3 as on Cav2.2.

According to experimental data however, the effective Gβγ binding site in Cav2.3 is the C-terminus, while the I-II loop also has Gβγ binding properties (chapter 4.2.3, Figs. 25A,D) (Qin et al. 1997; Berrou et al. 2001). There is no evidence for N-terminal binding of Gβγ in Cav2.3, contradicting the AlphaFold prediction. Looking at the α-helix sequences of Cav2.x, the basic K in Cav2.3 instead of the apolar M/I could potentially be a factor.

A

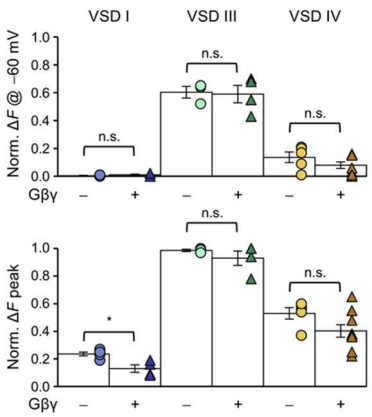

https://doi.org/10.1126/sciadv.adp6665

B

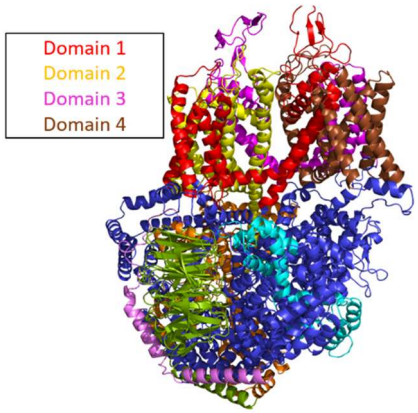

C

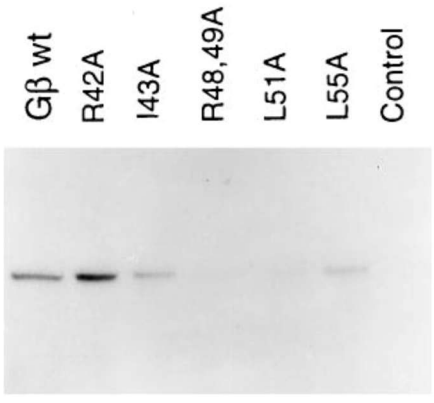

https://doi.org/10.1074/jbc.272.30.18801

D

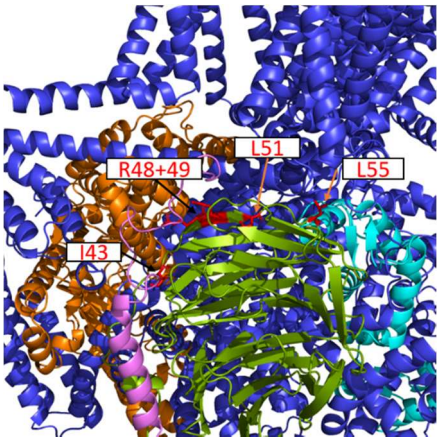

Figure 24 VSD I and CaM

The effects of Gβ1γ2 on voltage-sensing domains (VSD) I, III and IV consist of the S1-4 α-helices of the domain, while α-helices S5 and S6 build the pore. VSD II was excluded because it did not show ΔF, even at high voltages. In the resting state Gβ1γ2 did not cause significant changes in ΔF. In the active state ΔF for VSD I and VSD IV is significantly lower in the presence of Gβ1γ2, while ΔF for VSD III is not significantly lower in the presence of Gβ1γ2 (Fig 24A).

VSD I in the activated state was reduced to 13+-3% activation from 24+-1% by the presence of Gβ1γ2.

VSD III in the activated state was reduced to 93+-5% activation from 99+-1% activation by Gβ1γ2.

VSD IV in the activated state was reduced to 40+-5% activation from 53+-4% activation by Gβ1γ2.

Since VSD I is inhibited the most by Gβ1γ2, Gβ1γ2 might directly interact with VSD I and potentially VSD IV.

VSD II seems to have a different function than voltage sensing in Cav2 channels due to the lack of ΔF (Nilsson et al. 2024).

In the AlphaFold prediction (Fig. 24B) the VSDs and the pore building compartments are clearly distinguishable. Gβ1γ2 is located right below VSD I and proximity is given but not necessarily binding. Gβ1γ2 seems to bind the N-terminus which leads into VSD I, which could explain the strongest effect on VSD I. Interestingly VSD II is the VSD with the furthest distance to Gβ1γ2, potentially explaining the lack of effect. In the prediction the spatial separation between VSD IV and Gβ1γ2 is too far for direct interaction, but VSD IV is located closer to VSD I than VSD III is, potentially explaining the effect of Gβ1γ2 on VSD IV. The same distance applies to VSD II but it does not seem to be a voltage sensing component in Cav2.x channels.

Basic arginine residues and hydrophobic leucine and isoleucine residues of Gβ1 (Gβ1γ2) that are in the designated CaM-binding area of Gβ subunits (residues 40-63) were mutated to alanine and then their ability to bind CaM was observed and compared to the wild type (Fig. 24C). While R42A kept its Cam-binding ability, the other point mutations lost their CaM-binding abilities to different degrees. R48A, R49A and L51A showed the strongest loss of function (Liu et al. 1997).

In the AlphaFold prediction (figure 24D) those 3 residues are facing away from CaM and L55 shows superior proximity. The position of Gβ1γ2 is similar in the predictions for both the complex with calmodulin and without. The G protein is located in proximity to an N-terminal helix (49-59) and sits below VSD1 with high confidence in every prediction (with or without CaM).

4.2.2 AID and QxxER

A

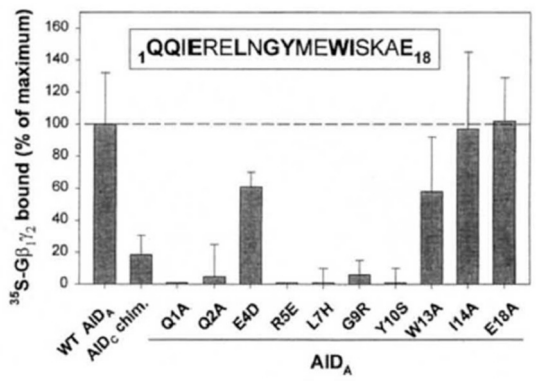

https://doi.org/10.1038/385446a0

B

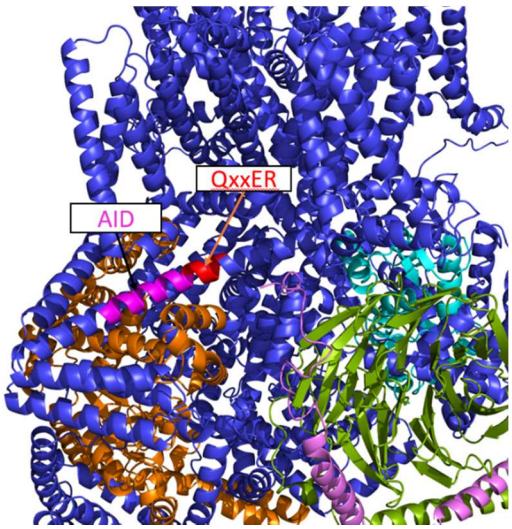

Cav2.2

C

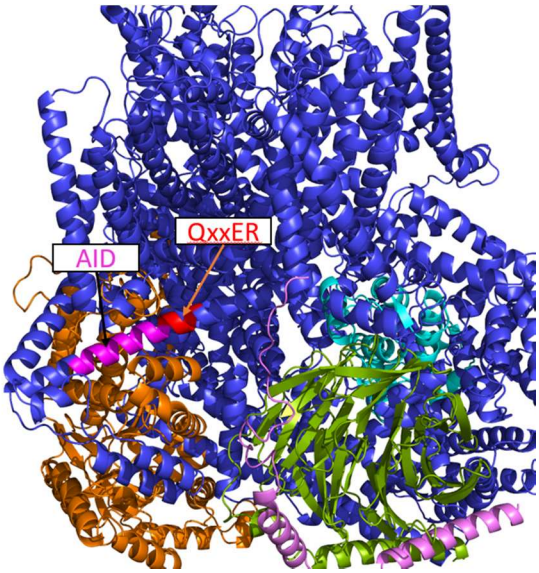

Cav2.1

D

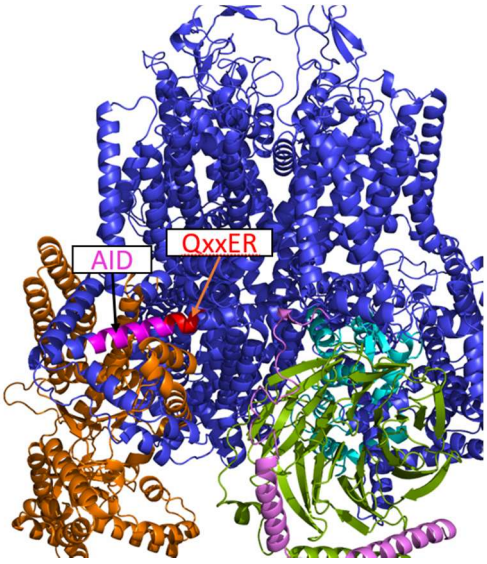

Cav2.3

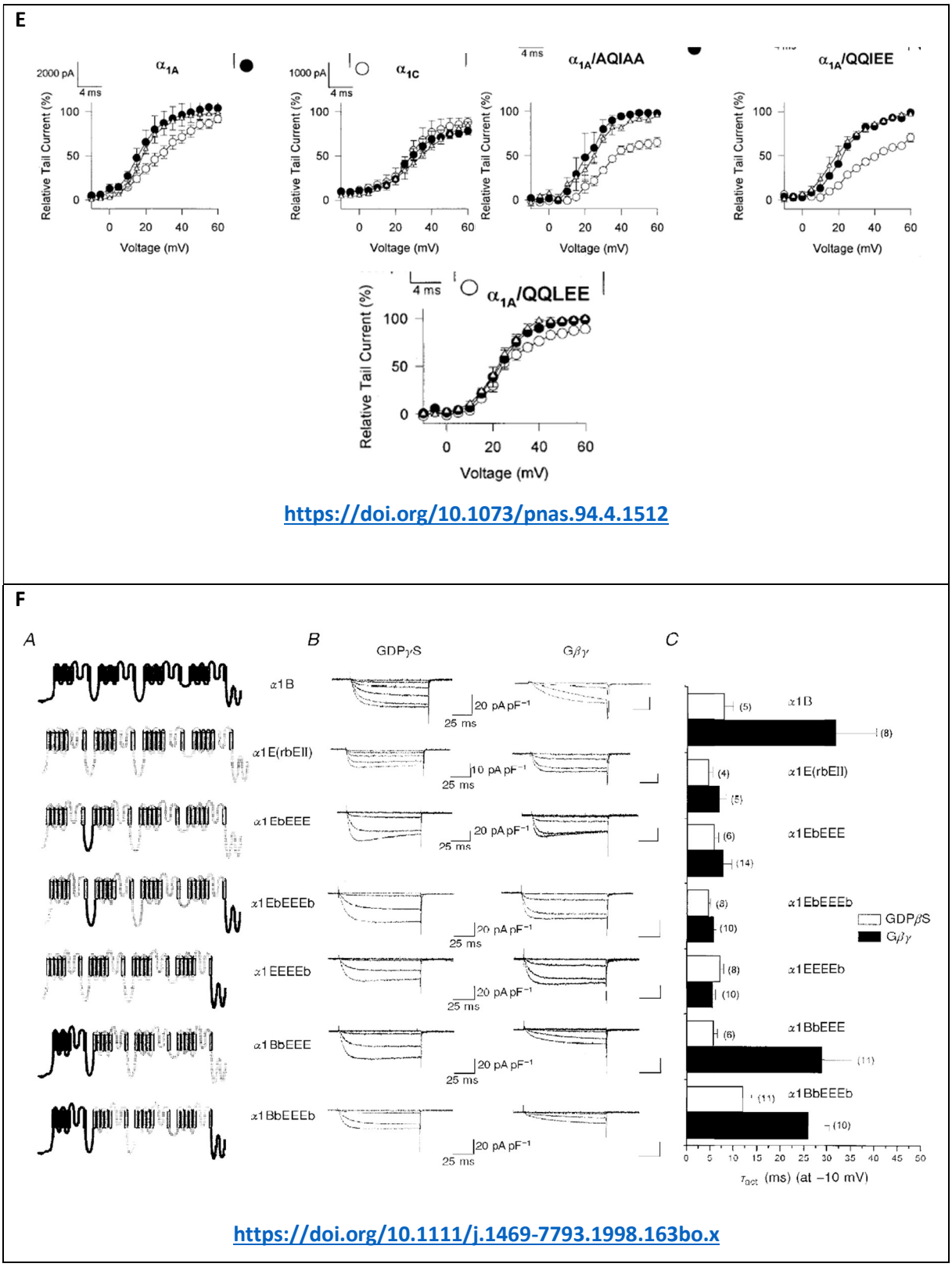

https://doi.org/10.1073/pnas.94.4.1512

https://doi.org/10.1111/j.1469-7793.1998.163bo.x

Figure 25 AID and QxxER

As mentioned in chapter 1.3.2 the 18 residue long AID is the β subunit binding sequence of the I-II loop with its first 5 residues being QxxER (Buraei and Yang 2010).

The 18 residues long AID sequence which is necessary for binding the β subunit (Figure 25A). It's also sufficient by itself to bind the β subunit. Single amino acids of the AID can differentiate between

different Cav channels (Cav1.x and Cav2.x) but **QQ** - **E** - - **L** - **GY** - - **WI** - - - **E** are universal. In Cav2.x the first 5 residues of the AID are QxxER (QQIER), which is a sequence generally linked to the binding of Gβ1γ2. The affinity of the β subunit to the AID is 10-20 times higher than the affinity of Gβ1γ2.

Point mutations were made in the AID of Cav2.2 in order to determine which residues are essential for Gβ1γ2 mediated inhibition. Q1A, Q2A, R5E, L7H, G9R and Y10S (from AID residues 1-18) resulted in complete loss of Gβ1γ2 binding. E4D, W13A, I14A and E18A however kept their Gβ1γ2 binding ability. Therefore residues 1-10 of the AID (QQ - - E - - L - - GY) were identified as essential for binding Gβ1γ2 to the AID (Fig. 25A).

Every Cav channel contains QxxE but only the Cav2.x family contains QxxER and only the Cav2.x family is inhibited by Gβ1γ2. Hence R5 of QxxER in the AID is essential for Gβ1γ2 mediated inhibition, proven by R5E in figure 24A (Waard et al. 1997).

The residues of AID including QxxER (QQIER) in Cav2.x channels are:

- Cav2.1: 383-400 → **QQ**I**E**RE**L**N**GY**ME**WI**SKA**E** (Fig. 25C)
- Cav2.2: 379-396 → **QQ**I**E**RE**L**N**GY**LE**WI**FKA**E** (Fig. 25B)
- Cav2.3: 374-391 → **QQ**I**E**RE**L**N**GY**RA**WI**DKA**E** (Fig. 25D)

The 18 residue long AID of Cav2.x channels differentiate in only 3 residues. In every AlphaFold prediction the AID is confidently predicted to be part of an α-helix, with or without Cavβ (Figs 25B-D). Furthermore as mentioned in chapters 1.3.2.2 and 1.3.2.3 the AID can also bind Gβγ. However in the AlphaFold predictions proximity from Gβ1γ2 to the AID is not given and no GBP is formed (Figs 25B-D). Therefore AlphaFold predicts Gβ1γ2 to solely bind the N-terminus.

However G-protein modulation (version of Gβγ not specified) occurs in Cav2.1 (α1a) and not in Cav1.2 (α1c) when induced by GTP[γS] (Fig. 25E). Point mutations were induced into the QQIER (QxxER) sequence of Cav2.1 in order to identify the residues responsible. Mutating this sequence to AQIAA and QQIEE did not abolish G-protein modulation, while the mutated sequence QQLEE showed drastically increased G-protein modulation. Consequently the I of QQIER was identified as a crucial determinant of G-protein modulation in Cav2.1. Ergo mutating the Gβγ binding QxxER sequence of the I-II linker of Cav2.1 affects G-protein modulation, supporting the idea that the I-II linker binding Gβγ is involved in Gβγ mediated inhibition (Herlitze et al., n.d.)

According to the AlphaFold prediction for Cav2.1 only the N-terminal α-helix is a binding site for Gβ1γ2 (Fig. 25C). There is no experimental evidence of Gβγ binding the Cav2.1 N-terminus but combining experimental data knowledge with the AlphaFold prediction could theoretically support the idea of forming a GBP in Cav2.1. Furthermore the AID of Cav2.1 and Cav2.2 only differ in 2/18 residues and the N-terminal α-helix in 1/11. The motifs are mostly similar, meaning that Gβ1γ2 binding properties of Cav2.2 motifs and Cav2.1 motifs also could be similar. Proof for both I-II loops binding Gβ1γ2 already

exists but proof of the Cav2.1 N-terminal binding Gβ1γ2 is currently not available. In chapter 1.3.2.2 it is also mentioned that Gβγ can bind Cav2.1 when Cavβ is also bound despite certain Gβγ binding residues being blocked (Buraei and Yang 2010). Having the N-terminus as another binding site could be a possible explanation.

Furthermore an experiment conducted by Stephens et al. (Fig. 25F) demonstrates that transferring the first 483 residues (N-terminus, Domain I and I-II loop) of Cav2.2 into Cav2.3 results in slower activation kinetics, since Cav2.2 is modulated stronger by Gβ1γ2 than Cav2.3 is. In this experiment Cavα, Cavβ2 and α2δ were expressed in COS-7 cells with Gβ1γ2. Transferring only the I-II loop and or the C-terminal of cav2.2 did not result in meaningful changes of activation kinetics. Therefore the I-II loop of Cav2.2 by itself does not induce Gβ1γ2 mediated inhibition. The combination of N-terminus, Domain I and I-II loop of Cav2.2 cause Gβ1γ2 mediated inhibition together (Stephens et al. 1998).

There is conflicting data on Gβγ mediated inhibition in channels after replacing solely the I-II loop with other I-II loops, but the common result is that they do not completely abolish Gβγ mediated inhibition, even when the I-II loop of Cav1.2 (not modulated by Gβ1γ2) is transferred. This suggests that other parts of Cav2.x channels are also involved, being the N-terminus and Domain I (Stephens et al. 1998). It has to be mentioned however that this paper handles the N-terminus as a part of Domain I and that the N-terminus without the rest of Domain I was not transferred.

This data provided by Stephens et al. therefore supports the involvement of both the N-terminus and the I-II loop in Gβ1γ2 mediated inhibition, further supporting the idea of the GBP formation.

Additionally transferring the C-terminal of Cav2.2 into Cav2.3 did not result in meaningful changes. In fact the activation kinetics were slower when the C-terminal was not transferred, hinting at possible Gβγ binding properties of the C-terminus of Cav2.3 (chapter 4.2.3, Fig. 26A) (Stephens et al. 1998).

4.2.3 The individuality of Cav2.3

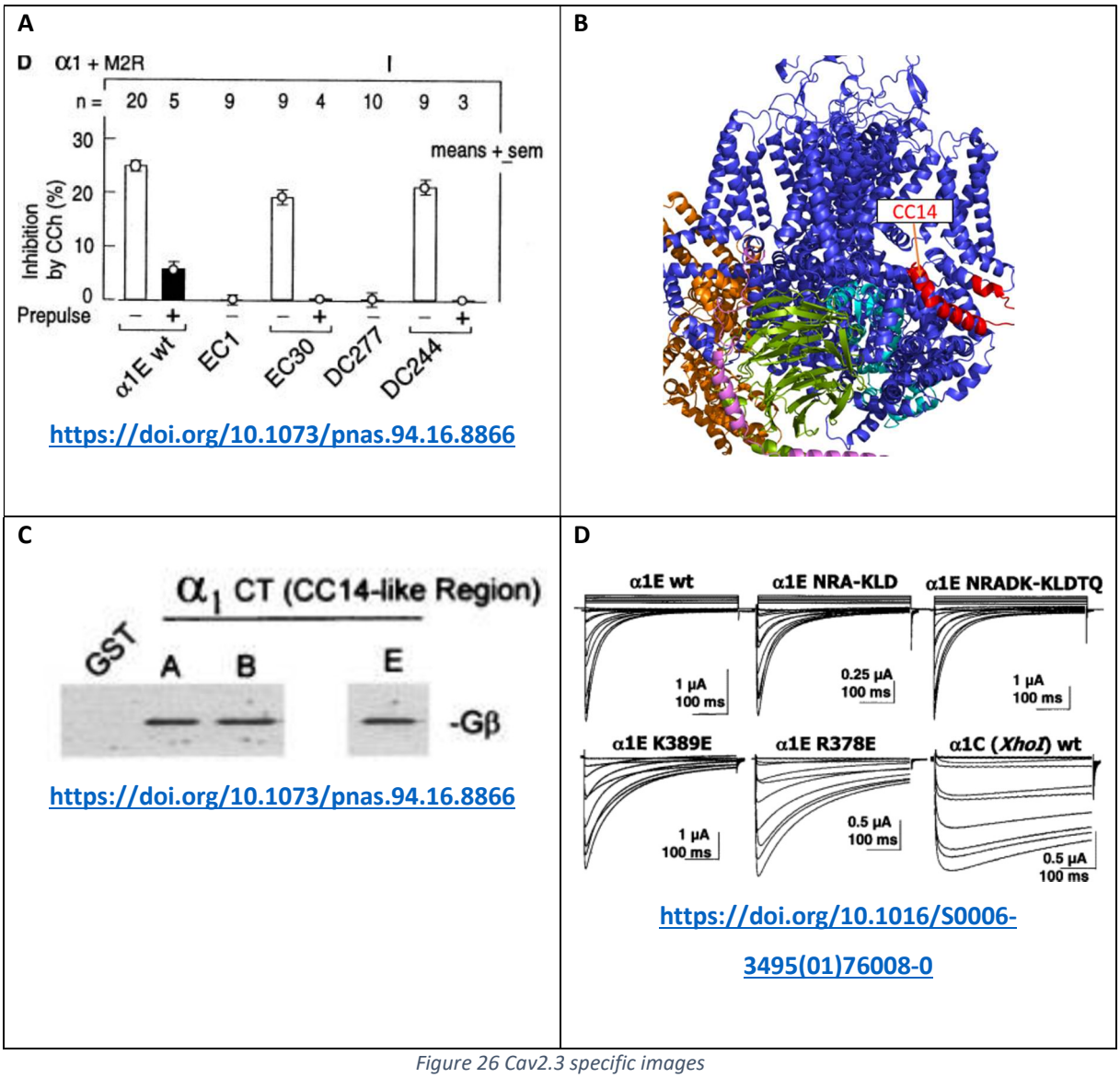

Figure 26 Cav2.3 specific images

In Cav2.3, the C-terminus is supposedly a major binding site for Gβγ, specifically a 38 residue long stretch labelled CC14. CC14 binds both the β2a[D4] and Gβγ, which compete for binding of CC14. Figure 25A contains multiple mutations and their effect on Gβγ mediated inhibition:

1. EC1 is Cav2.3 with the C-terminus of Cav1.2, a channel that is not inhibited by Gβγ.
2. EC30 is Cav2.3 with the I-II loop of Cav1.2, a channel that is not inhibited by Gβγ.
3. DC277 has a C-terminus that is shortened by 277 residues and therefore does not have CC14.
4. DC244 has a C-terminus that is shortened by 244 residues and therefore has 35 of the 38 residues from CC14.

Gβγ mediated regulation by the GPCR "M2R" is abolished when the C-terminus is replaced but not when the I-II loop is replaced (Fig. 26A). Hence the C-terminus of Cav2.3 and not the I-II loop is responsible for Gβγ binding and the following inhibition of Cav2.3, despite the I-II loops ability to bind Gβγ (Qin et al. 1997).

Furthermore DC244 kept its inhibitory prowess while DC277 did not, demonstrating the relevance of specifically the 35 CC14 residues available in DC244 for Gβγ binding and the following inhibition in Cav2.3 (Qin et al. 1997).

Proximity of CC14 to Gβ1γ2 is given in the AlphaFold prediction without the β3 subunit but confidence is low and the folding of the C-terminus is likely not realistic. Therefore the prediction likely does not represent the real CC14 but the proximity is promising. In the prediction with the β3 subunit (Fig. 26B), distance to Gβ1γ2 is increased and the C-terminus is still predicted with low confidence. Combining these results, AlphaFold potentially predicts the ability of CC14 to bind Gβ1γ2 but not necessarily the presence of said binding. Due to differentiating results of the predictions with and without the β3 subunit the strength of the affinity is to be questioned but seems to be present.

The CC14 equivalent regions of Cav2.1 and Cav2.2 also have bovine brain-Gβγ binding capabilities, when the α1 subunit is linked to GST (Fig. 26C). However they have not been identified as main Gβγ binding sites but binding is possible (Qin et al. 1997).

In Cav2.2 however, deleting residues 1877-2338, which are almost the entire C-terminus, did not result in loss of GTPγS induced inhibition, voltage dependant facilitation and inhibition or in change of activation kinetics (Meza and Adams 1998). Residues 2257-2336 of Cav2.2 directly bind Gβγ but their deletion does not affect Gβγ mediated inhibition. The existence of this binding site improves affinity but is not mechanistically essential for inhibition (Li et al., n.d.). In Cav2.1 the C-terminus plays an indirect role in Gβγ mediated inhibition. Its tail binds PIP and stabilizes the Gβγ-sensitive inhibited state (Rousset et al. 2004). Therefore only in Cav2.3 does the C-terminus play a central role in Gβγ mediated inhibition.

Multiple mutations within the AID of the I-II loop of Cav2.3 were expressed in Xenopus oocytes in the presence of the other 2 Cav2.3 subunits. Whole-cell currents in the presence of Ba2+ post EGTA injection demonstrate that R378 has a stronger effect on Gβγ mediated inhibition than other residues within the AID (Fig. 26D). Triple, quadruple and quintuple mutants failed to affect inactivation kinetics, while R378E and R378D resulted in drastically slower inactivation. K389E also resulted in slower inactivation but to a much smaller degree (Berrou et al. 2001).

Other point mutations of R378 showed different effects. Positively charged K instead of the positively charged R did not affect inactivation kinetics, while negatively charged D and E drastically slowed inactivation. Mutations with neutral amino acids differentiated from each other. R378A is similar to 378K while R378G is similar to R378D/E. R378Q slowed inactivation kinetics but only to an intermediate extent (Berrou et al. 2001).

Unlike the deletion of CC14, mutations within the AID did not abolish Gβγ mediated inhibition, but did cause slower inactivation kinetics. Therefore the C-terminus seems to be the main binding site for inhibition via Gβγ (Berrou et al. 2001).

The AlphaFold predictions for Cav2.3 always predict Gβ1γ2 binding at the N-terminus but currently there's no experimental proof for said interaction. However the basic K residue in the N-terminal α-helix of Cav2.3 (chapter 4.2.1) could potentially disrupt N-terminal binding of Gβγ and the GBP formation, although this is not predicted to be the case by AlphaFold. Only the C-terminus and I-II loop are proven to bind Gβγ and the C-terminus seems to be the essential motif. As mentioned in chapter 4.2.2, the I-II loop can bind Gβγ but it's not necessary for inhibition, meaning that the N-terminus (and potentially domain 1) suffice for Gβγ mediated inhibition in Cav2.2. In Cav2.3 the I-II loop also has Gβγ binding properties but isn't necessary for Gβγ mediated inhibition, the C-terminus is. Combining experimental data with the AlphaFold prediction could mean the following 2 things:

1. The AlphaFold prediction for Cav2.3- Gβ1γ2 is simply not admissible.
2. It could be insinuated that potentially the GBP of Cav2.3 is formed from 3 components, the N-terminus, I-II loop and C-terminus. The N-terminal α-helix and AID are mostly similar to Cav2.2 (chapters 4.2.1 and 4.2.2). Whether the C-terminus constitutes the sole functional interaction site remains uncertain. However the presence of additional regions interacting with Gβγ in other CaV2.x channels, the reported I-II loop interaction in CaV2.3 and AlphaFold predicting N-terminal binding suggest that CaV2.3 may employ a more distributed Gβγ interaction surface.

Cav2.3 is inhibited by Gβγ to a lesser extent than Cav2.1 and Cav2.2 (Berecki et al. 2014), which could be related to a different binding site or potentially by the necessity of another motif for the formation of the GBP. This is just a theory however and due to the low confidence prediction of the important C-terminus, the Cav2.3- Gβ1γ2 AlphaFold predictions are likely not representative of the real channel and interaction and therefore not admissible.

4.2.4 I-II loop mutations

Certain mutations in the I-II loop of Cav2.2 affect Gβ1γ2 mediated inhibition and similar residues can be found in similar locations in Cav2.1 and Cav2.3.

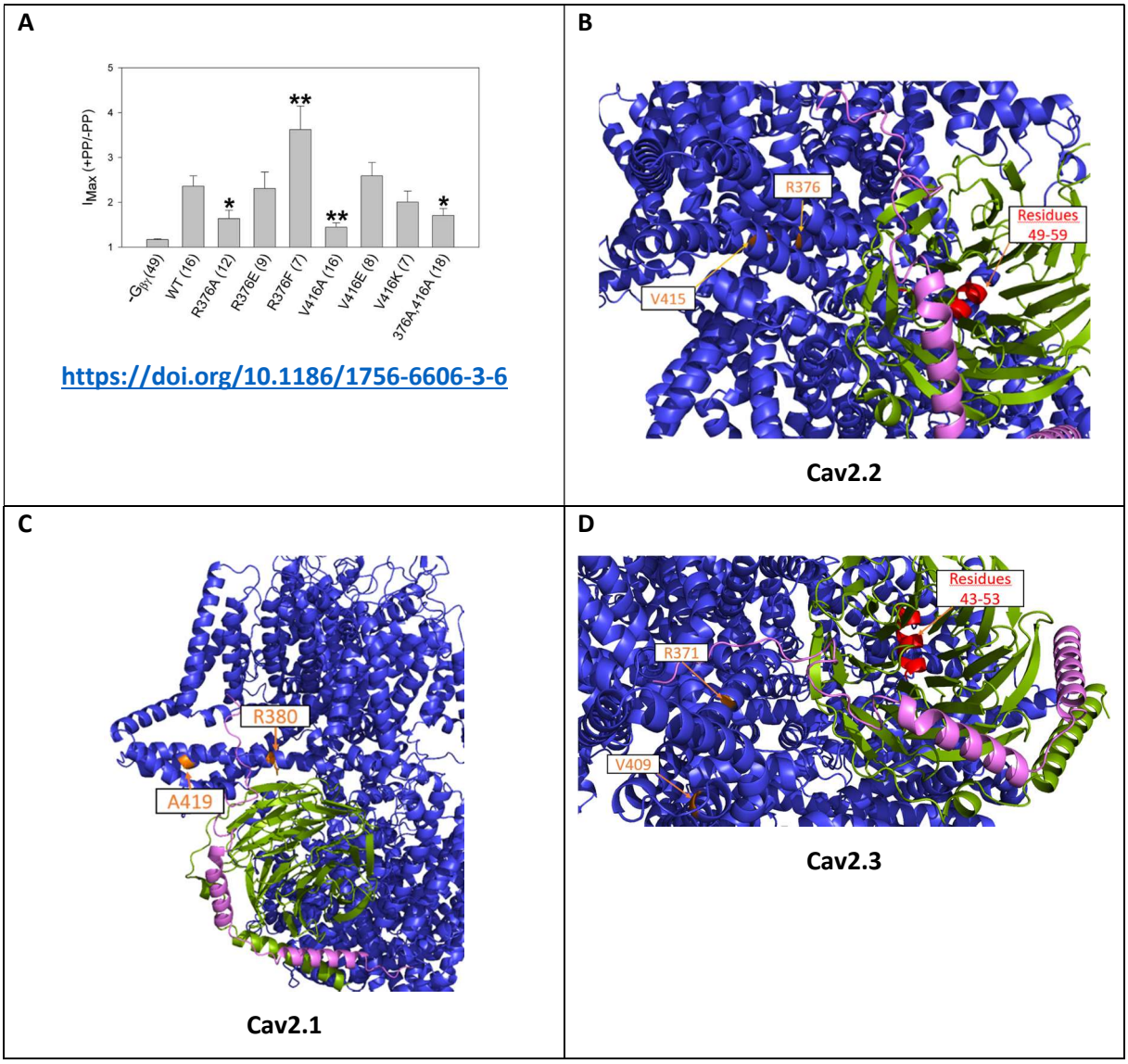

Figure 27 I-II loop mutations

Mutations introduced in the in the I-II loop of rat CACNA1B (HEK tsA-201 cells) affect Gβ1γ2 modulation (Figure 27A). Point mutations R376A and V416A significantly reduced inhibiting effects of Gβ1γ2. Having both mutations at the same time showed similar levels of reduced inhibition to only having one of those 2 point mutations. R376F on the other hand resulted in gain of function for Gβ1γ2 mediated inhibition, supporting the importance of R376 in Cav2.2 (R376F might create a more stable binding pocket by eliminating one of the 8 positive charges) (Tedford et al. 2010).

Since the I-II loop of CACNA1B is able to interact with the N-terminus of CACNA1B, the effect of R376 on Gβ1γ2 mediated inhibition could be of indirect nature by affecting the binding of the I-II loop to the

N-terminus. R376 is 3 residues away from the AID (379-396). According to Tedford et al., the AID by itself should form an α-helix (Tedford et al. 2010).

Residue 376 shows confidence in the AlphaFold prediction (Fig. 27B) and faces away from Gβ1γ2, supporting the idea of an indirect affect potentially via affecting the GBP. However, the AlphaFold prediction shows that R376 it is part of an α-helix (366-408). Residues 366, 367 and 408, which form the end of this helix show low confidence, but the other amino acids show confidence, contradicting the idea of 3 amino acids separating the α-helix and R376.

V416 is located at position 415 in the AlphaFold model and is part of a very low confidence stretch and therefore not admissible (Fig. 27B).

The equivalent residues of Cav2.1. In Cav2.2 the linker contains RRQQQI at residues 376-381 while Cav2.1 contains RRQQQI at residues 380-385, 4 positions further than in Cav2.2 (Figs 27B+C). Therefore the effects of mutations R376E (reduced Gβ1γ2 mediated Inhibition) and R376F (increased Gβ1γ2 mediated inhibition) in Cav2.2 could potentially be replicated by Cav2.1 point mutations R380E and R380F.

V415 from Cav2.2 however cannot be found in Cav2.1. Cav2.2 contains EVL at residues 414-416, Cav2.1 however contains EAL at residues 418-420. Therefore valine is replaced by alanine (Figs 27 B+C).

V415A (or V416A) in Cav2.2 causes loss of Gβ1γ2 mediated inhibition (Fig. 25A) (Tedford et al. 2010), which is the exact replacement we can observe in Cav2.1 but moved by 4 positions → V419A (Fig. 27C).

In rat CaV2.1 channels, splice variants containing a V421 insertion in the I–II loop exhibited enhanced Gβγ mediated inhibition (Bourinet et al. 1999). This doesn't put V at position 419 but it shoes that the presence of V in this area of the I-II loop can affect Gβγ mediated inhibition.

Gβ1γ2 inhibits Cav2.2 to a greater extent than Cav2.1 (Currie and Fox 1997) and Gβγ dissociates more slowly from CaV2.2 than from CaV2.1, consistent with more persistent G-protein mediated inhibition of CaV2.2 (Zhang et al. 1996). The A instead of V in Cav2.1 could potentially be a cause for that since V415A (or V416A) causes loss of inhibition in Cav2.2.

RRQQQI is located at residues 371-376 and EVL is located at residues 408-410 in Cav2.3 (Figure 25D).

Listing of residues:

- Cav2.1: RRQQQI 380-385; EAL 418-420 (Fig. 27C)
- Cav2.2: RRQQQI 376-381; EVL 414-416 (Fig. 27B)
- Cav2.3: RRQQQI 371-376; EVL 408-410 (Fig. 27D)

Despite having the EVL sequence, Cav2.3 is inhibited by Gβγ to a lesser extent than Cav2.1 and Cav2.2 (Berecki et al. 2014). This could be due to binding site differences which are further explored in the Cav2.3 chapter (chapter 4.2.3).

4.2.5 Cav2.1 VSD mutations

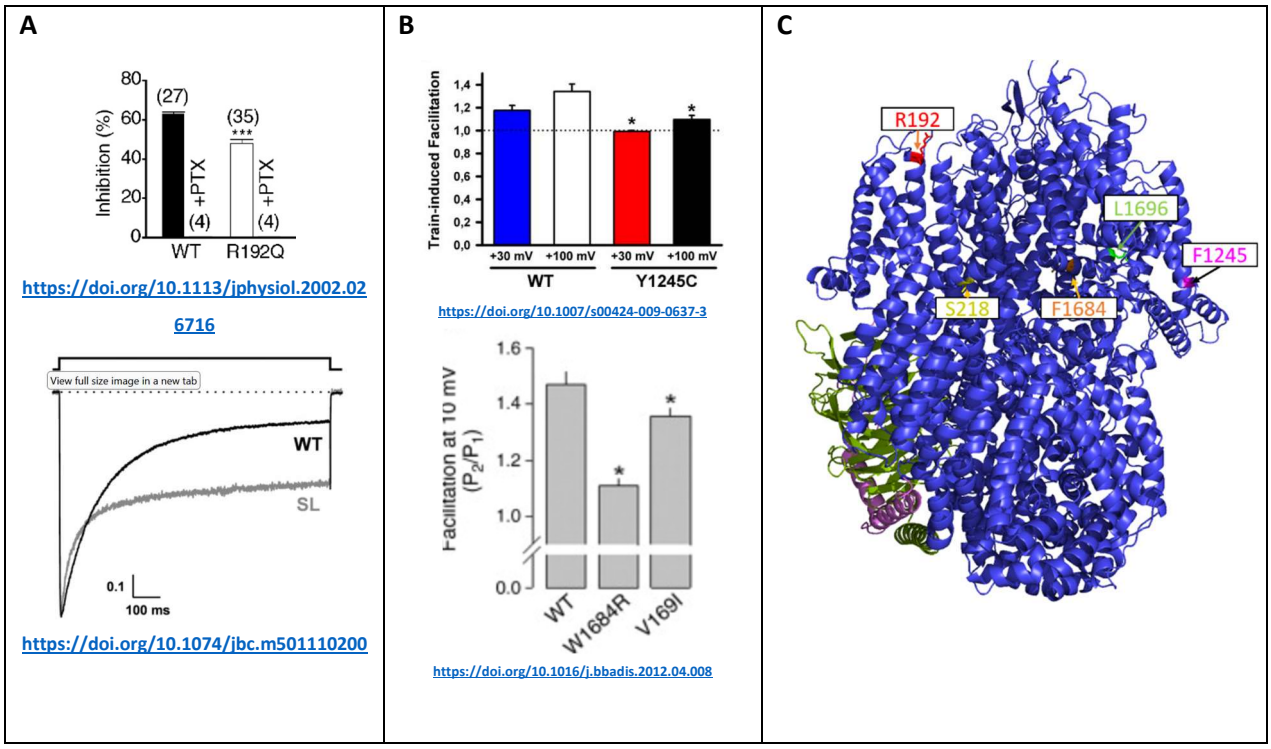

Figure 28 Cav2.1 specific images

Multiple mutations that affect Gβγ mediated inhibition of Cav2.1, but not at the binding site and therefore just affect inhibition, not binding (Figures 28A+B). The affected residues are marked in the AlphaFold prediction (Fig. 28C):

1. R192Q in S4 of VSD1 results in gain of function (Melliti et al. 2003)
2. S218L causes strong gain of function (Tottene et al. 2005)
3. Y1245C in VSD III causes gain of function (Serra et al. 2009)
4. W1684R in VSD IV causes gain of function (Garza-López et al. 2012)
5. V1696I in VSD IV causes gain of function (Garza-López et al. 2012)

5 Conclusion

The Cav2.2 model showed the highest level of agreement with available experimental evidence. The C-terminus is predicted with low confidence for all 3 channels but the Cav2.2 model could be confidently used in simulations, due to lack of evidence for the involvement of the C-terminus. The N-terminal binding site correlates with experimental data and in a mobile simulation instead of a static prediction like AlphaFold, the involvement of the I-II loop (specifically the AID) could potentially be observed.

There's no experimental evidence for the predicted N-terminal binding site in Cav2.1, but due to the similarity in sequence (1/11 are different) to Cav2.2, an N-terminal binding site is plausible. However there is evidence of Gβγ binding the AID, specifically the QxxER sequence, which is also similar in sequence to Cav2.2 (2/18 are different) and all the different residues are nonpolar and hydrophobic in both cav2.1 and Cav2.2. Therefore similarities in Gβ1γ2 binding for Cav2.1 and Cav2.2 appear plausible and are predicted by AlphaFold. The Cav2.1 prediction may also be suitable for further simulations, although the question of N-terminal binding should be experimentally tested. This could also play a role in supporting or disproving the formation of the GBP in Cav2.x channels (at least for Cav2.1 and Cav2.2), which is already supported by evidence of N-terminus and I-II loop involvement in Cav2.2.

Interestingly different residues of the QxxER sequence in Cav2.1 and Cav2.2 seem to be important for Gβγ binding, suggesting that identical residues may be affected differently by the structural context of the channel. However this could also be the result of differently structured experiments

Cav2.1 is modulated by Gβγ to a lesser extent than Cav2.2, potentially due to the V to A exchange in the I-II loop, which is a mutation proven to reduce Gβ1γ2 mediated inhibition in Cav2.2. The presence of V in that area is also proven to increase Gβγ modulation in rat Cav2.1. This residue change by itself could potentially explain the differences of modulation strength in Cav2.1 and Cav2.2.

The Cav2.3 model is likely not admissible due to the low confidence prediction of the C-terminus, which is the main Gβγ binding site in Cav2.3 according to experimental data. There is also no proof for the predicted N-terminal binding site. It only differentiates in 1/9 residues from Cav2.1 and Cav2.2, but that residue is positively charged instead of nonpolar. However there is proof of the I-II loop having binding capabilities and the AID differentiates in 3/18 residues from Cav2.1 and Cav2.2 and one of the Cav2.3 residues is nonpolar instead of negatively charged. These changes in charge could affect binding affinity, potentially explaining why Cav2.3 is inhibited to a lesser extent than Cav2.1 and Cav2.2. The N-terminus of Cav2.2 is proven to be modulated to a stronger extent than the N-terminus of Cav2.3. Said lower affinity could also explain the increased involvement of the C-terminus, since its Gβγ binding affinity could now be similar or higher than the affinity of the N-terminus or the I-II loop.

Cav2.3 is modulated the least out of these 3 channels, insinuating that it could be of the lowest importance for GNB1-E. Potential future simulations with the models of Cav2.1 and Cav2.2 are a promising start for testing the involvement of Cav2.x channels in GNB1-E and potential treatment. Since altered Gβγ signaling is believed to contribute to the pathophysiology of GNB1 encephalopathy, the identification of Cav2.2 as the most structurally supported model system may facilitate future studies investigating the effects of disease-associated GNB1 variants on Cav channel regulation.

6 References

Abramson, Josh, Jonas Adler, Jack Dunger, et al. 2024. 'Accurate Structure Prediction of Biomolecular Interactions with AlphaFold 3'. *Nature* 630 (8016): 493–500. https://doi.org/10.1038/s41586-024-07487-w.

Andrade, Arturo, Alejandro Sandoval, Norma Oviedo, Michel De Waard, David Elias, and Ricardo Felix. 2007. 'Proteolytic Cleavage of the Voltage-gated Ca^{2+} Channel α_2 δ Subunit: Structural and Functional Features'. *European Journal of Neuroscience* 25 (6): 1705–10. https://doi.org/10.1111/j.1460-9568.2007.05454.x.

Ben-Johny, Manu, and David T. Yue. 2014. 'Calmodulin Regulation (Calmodulation) of Voltage-Gated Calcium Channels'. *Journal of General Physiology* 143 (6): 679–92. https://doi.org/10.1085/jgp.201311153.

Berecki, Géza, Jeffrey R. McArthur, Hartmut Cuny, Richard J. Clark, and David J. Adams. 2014. 'Differential Cav2.1 and Cav2.3 Channel Inhibition by Baclofen and α-Conotoxin Vc1.1 via GABAB Receptor Activation'. *Journal of General Physiology* 143 (4): 465–79. https://doi.org/10.1085/jgp.201311104.

Berrou, L., G. Bernatchez, and L. Parent. 2001. 'Molecular Determinants of Inactivation within the I-II Linker of α1E (CaV2.3) Calcium Channels'. *Biophysical Journal* 80 (1): 215–28. https://doi.org/10.1016/S0006-3495(01)76008-0.

Bourinet, Emmanuel, Tuck W. Soong, Kathy Sutton, et al. 1999. 'Splicing of α1A Subunit Gene Generates Phenotypic Variants of P- and Q-Type Calcium Channels'. *Nature Neuroscience* 2 (5): 407–15. https://doi.org/10.1038/8070.

Buraei, Zafir, and Jian Yang. 2010. 'The β Subunit of Voltage-Gated Ca^{2+} Channels'. *Physiological Reviews* 90 (4): 1461–506. https://doi.org/10.1152/physrev.00057.2009.

Burgess, Daniel L., Julie M. Jones, Miriam H. Meisler, and Jeffrey L. Noebels. n.d. *Mutation of the Ca21 Channel b Subunit Gene Cchb4 Is Associated with Ataxia and Seizures in the Lethargic (Lh) Mouse*.

Caminski, Emanuelle Sistherenn, Flavia Tasmin Techera Antunes, Ivana Assis Souza, Eliane Dallegrave, and Gerald W. Zamponi. 2022. 'Regulation of N-Type Calcium Channels by Nociceptin Receptors and Its Possible Role in Neurological Disorders'. *Molecular Brain* 15 (1): 95. https://doi.org/10.1186/s13041-022-00982-z.

Cantí, Carles, Karen M. Page, Gary J. Stephens, and Annette C. Dolphin. 1999. 'Identification of Residues in the N Terminus of α1B Critical for Inhibition of the Voltage-Dependent Calcium Channel by Gβγ'. *The Journal of Neuroscience* 19 (16): 6855–64. https://doi.org/10.1523/JNEUROSCI.19-16-06855.1999.

Catterall, W. A. 2011. 'Voltage-Gated Calcium Channels'. *Cold Spring Harbor Perspectives in Biology* 3 (8): a003947–a003947. https://doi.org/10.1101/cshperspect.a003947.

Currie, Kevin P. M., and Aaron P. Fox. 1997. 'Comparison of N- and P/Q-Type Voltage-Gated Calcium Channel Current Inhibition'. *The Journal of Neuroscience* 17 (12): 4570–79. https://doi.org/10.1523/JNEUROSCI.17-12-04570.1997.

Da Silva, Jorge Diogo, Marta Daniela Costa, Bruno Almeida, Fátima Lopes, Patrícia Maciel, and Andreia Teixeira-Castro. 2021. 'Case Report: A Novel GNB1 Mutation Causes Global Developmental Delay With Intellectual Disability and Behavioral Disorders'. *Frontiers in Neurology* 12 (September): 735549. https://doi.org/10.3389/fneur.2021.735549.

Davies, Anthony, Ivan Kadurin, Anita Alvarez-Laviada, et al. 2010. 'The α_2 δ Subunits of Voltage-Gated Calcium Channels Form GPI-Anchored Proteins, a Posttranslational Modification Essential for Function'. *Proceedings of the National Academy of Sciences* 107 (4): 1654–59. https://doi.org/10.1073/pnas.0908735107.

DeMaria, Carla D., Tuck Wah Soong, Badr A. Alseikhan, Rebecca S. Alvania, and David T. Yue. 2001. 'Calmodulin Bifurcates the Local Ca2+ Signal That Modulates P/Q-Type Ca2+ Channels'. *Nature* 411 (6836): 484–89. https://doi.org/10.1038/35078091.

Dolphin, Annette C. 2013. 'The A2δ Subunits of Voltage-Gated Calcium Channels'. *Biochimica et Biophysica Acta (BBA) - Biomembranes* 1828 (7): 1541–49. https://doi.org/10.1016/j.bbamem.2012.11.019.

Dong, Yanli, Yiwei Gao, Shuai Xu, et al. 2021. 'Closed-State Inactivation and Pore-Blocker Modulation Mechanisms of Human CaV2.2'. *Cell Reports* 37 (5): 109931. https://doi.org/10.1016/j.celrep.2021.109931.

Fernández-Quintero, Monica L., Yousra El Ghaleb, Petronel Tuluc, Marta Campiglio, Klaus R. Liedl, and Bernhard E. Flucher. 2021. 'Structural Determinants of Voltage-Gating Properties in Calcium Channels'. *eLife* 10 (March): e64087. https://doi.org/10.7554/eLife.64087.

Ford, Carolyn E., Nikolai P. Skiba, Hyunsu Bae, et al. 1998. *Molecular Basis for Interactions of G Protein By Subunits with Effectors*. 280.

Garza-López, Edgar, Alejandro Sandoval, Ricardo González-Ramírez, et al. 2012. 'Familial Hemiplegic Migraine Type 1 Mutations W1684R and V1696I Alter G Protein-Mediated Regulation of CaV2.1 Voltage-Gated Calcium Channels'. *Biochimica et Biophysica Acta (BBA) - Molecular Basis of Disease* 1822 (8): 1238–46. https://doi.org/10.1016/j.bbadis.2012.04.008.

Gurnett, Christina A., Ricardo Felix, and Kevin P. Campbell. 1997. 'Extracellular Interaction of the Voltage-Dependent Ca2+ Channel A2δ and A1 Subunits'. *Journal of Biological Chemistry* 272 (29): 18508–12. https://doi.org/10.1074/jbc.272.29.18508.

Hawrylycz, Michael J., Ed S. Lein, Angela L. Guillozet-Bongaarts, et al. 2012. 'An Anatomically Comprehensive Atlas of the Adult Human Brain Transcriptome'. *Nature* 489 (7416): 391–99. https://doi.org/10.1038/nature11405.

Herlitze, Stefan, Gregory H. Hockerman, Todd Scheuer, and William A. Catterall. n.d. *Molecular Determinants of Inactivation and G Protein Modulation in the Intracellular Loop Connecting Domains I and II of the Calcium Channel α1A Subunit*.

Ikeda, Stephen R. 1996. *Voltage-Dependent Modulation of N-Type Calcium Channels by G-Protein Py Subunits*. 380.

Jeziorski, Michael C., and Robert M. Greenberg. 2006. 'Voltage-Gated Calcium Channel Subunits from Platyhelminths: Potential Role in Praziquantel Action'. *International Journal for Parasitology* 36 (6): 625–32. https://doi.org/10.1016/j.ijpara.2006.02.002.

Jumper, John, Richard Evans, Alexander Pritzel, et al. 2021. 'Highly Accurate Protein Structure Prediction with AlphaFold'. *Nature* 596 (7873): 583–89. https://doi.org/10.1038/s41586-021-03819-2.

Kjær, Christina, Oana Palasca, Guido Barzaghi, et al. 2023. 'Differential Expression of the B3 Subunit of Voltage-Gated Ca2+ Channel in Mesial Temporal Lobe Epilepsy'. *Molecular Neurobiology* 60 (10): 5755–69. https://doi.org/10.1007/s12035-023-03426-4.

Lacinova, Lubica, Robert Theodor Mallmann, Bohumila Jurkovičová-Tarabová, and Norbert Klugbauer. 2020. 'Modulation of Voltage-Gated Ca_V 2.2 Ca^{2+} Channels by Newly Identified Interaction Partners'. *Channels* 14 (1): 380–92. https://doi.org/10.1080/19336950.2020.1831328.

Li, Bin, Huijun Zhong, Todd Scheuer, and William A. Catterall. n.d. *Functional Role of a C-Terminal G -Binding Domain of Cav2.2 Channels*.

Liu, Mingyao, Bo Yu, Osamu Nakanishi, Thomas Wieland, and Melvin Simon. 1997. 'The Ca2+-Dependent Binding of Calmodulin to an N-Terminal Motif of the Heterotrimeric G Protein β Subunit *'. *Journal of Biological Chemistry* 272 (30): 18801–7. https://doi.org/10.1074/jbc.272.30.18801.

Lohmann, Katja, Ikuo Masuho, Dipak N. Patil, et al. 2017. 'Novel *GNB1* Mutations Disrupt Assembly and Function of G Protein Heterotrimers and Cause Global Developmental Delay in Humans'. *Human Molecular Genetics*, January 13, ddx018. https://doi.org/10.1093/hmg/ddx018.

Mayo, Sonia, Irene Gómez-Manjón, Ana Victoria Marco-Hernández, Francisco Javier Fernández-Martínez, Ana Camacho, and Francisco Martínez. 2023. 'N-Type Ca Channel in Epileptic Syndromes and Epilepsy: A Systematic Review of Its Genetic Variants'. *International Journal of Molecular Sciences* 24 (7): 6100. https://doi.org/10.3390/ijms24076100.

Melliti, Karim, Manfred Grabner, and Guy R. Seabrook. 2003. 'The Familial Hemiplegic Migraine Mutation R192q Reduces G-protein-mediated Inhibition of p/Q-type (Ca_v 2.1) Calcium Channels Expressed in Human Embryonic Kidney Cells'. *The Journal of Physiology* 546 (2): 337–47. https://doi.org/10.1113/jphysiol.2002.026716.

Meza, Ulises, and Brett Adams. 1998. 'G-Protein-Dependent Facilitation of Neuronal α_{1A} , α_{1B} , and α_{1E} Ca Channels'. *The Journal of Neuroscience* 18 (14): 5240–52. https://doi.org/10.1523/JNEUROSCI.18-14-05240.1998.

Mori, Masayuki X., Craig W. Vander Kooi, Daniel J. Leahy, and David T. Yue. 2008. 'Crystal Structure of the CaV2 IQ Domain in Complex with Ca2+/Calmodulin: High-Resolution Mechanistic Implications for Channel Regulation by Ca2+'. *Structure* (London, England : 1993) 16 (4): 607–20. https://doi.org/10.1016/j.str.2008.01.011.

Murakami, Manabu, Takayoshi Ohba, Feng Xu, et al. 2008. 'Modified Sympathetic Nerve System Activity with Overexpression of the Voltage-Dependent Calcium Channel B3 Subunit'. *Journal of Biological Chemistry* 283 (36): 24554–60. https://doi.org/10.1074/jbc.M802319200.

Nasvytis, Matas, Julija Čiauškaitė, and Giedrė Jurkevičienė. 2024. 'GNB1 Encephalopathy: Clinical Case Report and Literature Review'. *Medicina* 60 (4): 589. https://doi.org/10.3390/medicina60040589.

Nilsson, Michelle, Kaiqian Wang, Teresa Mínguez-Viñas, et al. 2024. 'Voltage-Dependent G-Protein Regulation of Ca_V 2.2 (N-Type) Channels'. *Science Advances* 10 (37): eadp6665. https://doi.org/10.1126/sciadv.adp6665.

Pang, Zhiping P., Peng Cao, Wei Xu, and Thomas C. Südhof. 2010. 'Calmodulin Controls Synaptic Strength via Presynaptic Activation of Calmodulin Kinase II'. *The Journal of Neuroscience* 30 (11): 4132–42. https://doi.org/10.1523/JNEUROSCI.3129-09.2010.

Parajuli, Laxmi Kumar, Chikako Nakajima, Akos Kulik, et al. 2012. 'Quantitative Regional and Ultrastructural Localization of the Ca_v 2.3 Subunit of R-Type Calcium Channel in Mouse Brain'. *The Journal of Neuroscience* 32 (39): 13555–67. https://doi.org/10.1523/JNEUROSCI.1142-12.2012.

Park, Cheon-Gyu, and Byung-Chang Suh. 2018. 'Modulation Mechanisms of Voltage-Gated Calcium Channels'. *Current Opinion in Physiology* 2 (April): 77–83. https://doi.org/10.1016/j.cophys.2018.01.005.

Petrovski, Slavé, Sébastien Küry, Candace T. Myers, et al. 2016. 'Germline De Novo Mutations in GNB1 Cause Severe Neurodevelopmental Disability, Hypotonia, and Seizures'. *The American Journal of Human Genetics* 98 (5): 1001–10. https://doi.org/10.1016/j.ajhg.2016.03.011.

Qin, Ning, Daniela Platano, Riccardo Olcese, Enrico Stefani, and Lutz Birnbaumer. 1997. 'Direct Interaction of Gβγ with a C-Terminal Gβγ-Binding Domain of the Ca^{2+} Channel α_1 Subunit Is Responsible for Channel Inhibition by G Protein-Coupled Receptors'. *Proceedings of the National Academy of Sciences* 94 (16): 8866–71. https://doi.org/10.1073/pnas.94.16.8866.

Revah-Politi, Anya, Tristan T. Sands, Sophie Colombo, David B. Goldstein, and Kwame Anyane-Yeboa. n.d. *GNB1 Encephalopathy*.

Rousset, Matthieu, Thierry Cens, Annie Gouin-Charnet, Frédérique Scamps, and Pierre Charnet. 2004. 'Ca2+ and Phosphatidylinositol 4,5-Bisphosphate Stabilize a Gβγ-Sensitive State of CaV2 Ca2+ Channels'. *Journal of Biological Chemistry* 279 (15): 14619–30. https://doi.org/10.1074/jbc.M313284200.

Serra, Selma A., Noèlia Fernàndez-Castillo, Alfons Macaya, Bru Cormand, Miguel A. Valverde, and José M. Fernández-Fernández. 2009. 'The Hemiplegic Migraine-Associated Y1245C Mutation in CACNA1A Results in a Gain of Channel Function Due to Its Effect on the Voltage Sensor and G-Protein-Mediated Inhibition'. *Pflügers Archiv - European Journal of Physiology* 458 (3): 489–502. https://doi.org/10.1007/s00424-009-0637-3.

Smrcka, A. V. 2008. 'G Protein Bγ Subunits: Central Mediators of G Protein-Coupled Receptor Signaling'. *Cellular and Molecular Life Sciences* 65 (14): 2191–214. https://doi.org/10.1007/s00018-008-8006-5.

Stephens, Gary J., Carles Cantí, Karen M. Page, and Annette C. Dolphin. 1998. 'Role of Domain I of Neuronal Ca^{2+} Channel A1 Subunits in G Protein Modulation'. *The Journal of Physiology* 509 (1): 163–69. https://doi.org/10.1111/j.1469-7793.1998.163bo.x.

Tedford, Hugo W., Alexandra E. Kisilevsky, Lucienne B. Vieira, Diego Varela, Lina Chen, and Gerald W. Zamponi. 2010. 'Scanning Mutagenesis of the I-II Loop of the Cav2.2 Calcium Channel Identifies Residues Arginine 376 and Valine 416 as Molecular Determinants of Voltage Dependent G Protein Inhibition'. *Molecular Brain* 3 (1): 6. https://doi.org/10.1186/1756-6606-3-6.

Tottene, Angelita, Francesca Pivotto, Tommaso Fellin, Tiziana Cesetti, Arn M. J. M. van den Maagdenberg, and Daniela Pietrobon. 2005. 'Specific Kinetic Alterations of Human CaV2.1 Calcium Channels Produced by Mutation S218L Causing Familial Hemiplegic Migraine and Delayed Cerebral Edema and Coma after Minor Head Trauma *'. *Journal of Biological Chemistry* 280 (18): 17678–86. https://doi.org/10.1074/jbc.M501110200.

Vendel, Andrew C., Mark D. Terry, Amelia R. Striegel, et al. 2006. 'Alternative Splicing of the Voltage-Gated Ca^{2+} Channel β_4 Subunit Creates a Uniquely Folded N-Terminal Protein Binding Domain with Cell-Specific Expression in the Cerebellar Cortex'. *The Journal of Neuroscience* 26 (10): 2635–44. https://doi.org/10.1523/JNEUROSCI.0067-06.2006.

Waard, Michel De, Hongyan Liu, Denise Walker, Victoria E. S. Scott, Christina A. Gurnett, and Kevin P. Campbell. 1997. 'Direct Binding of G-Protein Bλ Complex to Voltage-Dependent Calcium Channels'. *Nature* 385 (6615): 446–50. https://doi.org/10.1038/385446a0.

Wilson, Scott M., Peter T. Toth, Seog Bae Oh, et al. n.d. *The Status of Voltage-Dependent Calcium Channels in a1E Knock- Out Mice*.

Wootten, Denise, Arthur Christopoulos, Maria Marti-Solano, M. Madan Babu, and Patrick M. Sexton. 2018. 'Mechanisms of Signalling and Biased Agonism in G Protein-Coupled Receptors'. *Nature Reviews Molecular Cell Biology* 19 (10): 638–53. https://doi.org/10.1038/s41580-018-0049-3.

Yao, Xia, Shuai Gao, and Nieng Yan. 2024. 'Structural Biology of Voltage-Gated Calcium Channels'. *Channels* 18 (1): 2290807. https://doi.org/10.1080/19336950.2023.2290807.

Zamponi, Gerald W. 2017. 'A Crash Course in Calcium Channels'. *ACS Chemical Neuroscience* 8 (12): 2583–85. https://doi.org/10.1021/acschemneuro.7b00415.

Zamponi, Gerald W., and Kevin P. M. Currie. 2013. 'Regulation of CaV2 Calcium Channels by G Protein Coupled Receptors'. *Biochimica et Biophysica Acta (BBA) - Biomembranes* 1828 (7): 1629–43. https://doi.org/10.1016/j.bbamem.2012.10.004.

Zhang, Ji-Fang, Patrick T. Ellinor, Richard W. Aldrich, and Richard W. Tsien. 1996. 'Multiple Structural Elements in Voltage-Dependent Ca2+ Channels Support Their Inhibition by G Proteins'. *Neuron* 17 (5): 991–1003. https://doi.org/10.1016/S0896-6273(00)80229-9.

Zhu, Junliang, Hu Qiu, and Wanlin Guo. 2023. 'Probing Ion Binding in the Selectivity Filter of the Cav1.1 Channel with Molecular Dynamics'. *Biophysical Journal* 122 (3): 496–505. https://doi.org/10.1016/j.bpj.2022.12.037.